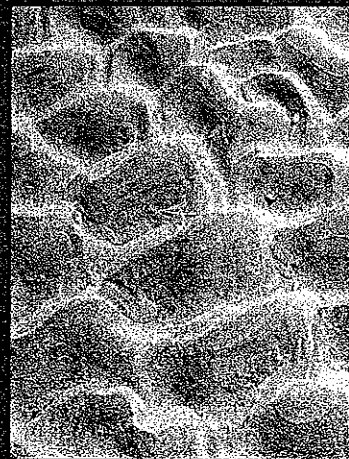


F-1301

c. 2

98206055

**SEDIMENT TRANSPORT IN ELLIOTT
BAY AND THE DUWAMISH RIVER,
SEATTLE: IMPLICATIONS TO
ESTUARINE MANAGEMENT**



GeoSea

Consulting

**SEDIMENT TRANSPORT IN ELLIOTT
BAY AND THE DUWAMISH RIVER,
SEATTLE: IMPLICATIONS TO
ESTUARINE MANAGEMENT**

**SEDIMENT TRANSPORT IN ELLIOTT BAY
AND THE DUWAMISH RIVER, SEATTLE:
IMPLICATIONS TO ESTUARINE MANAGEMENT**

By:

Patrick McLaren and Ping Ren
GeoSea Consulting (Canada) Ltd.,
#6-2810 Fulford-Ganges Road,
Salt Spring Island,
British Columbia,
Canada, V8K 1Z2

Prepared for:

Washington Department of Ecology, Toxics Cleanup Program

Funding for this project was provided by:

Elliott Bay/Duwamish Restoration Panel
U.S. Environmental Protection Agency, Region 10
NOAA Damage Assessment and Restoration Center Northwest
Washington Department of Natural Resources
Port of Seattle

This report presents the interpretation and conclusions of the authors. Because formal review has not been conducted, this document should be considered a technical report, not as official policy or recommendations of the funding organizations. Any comments regarding this report should be forwarded to:

Dr. Teresa Michelsen
Department of Ecology
Northwest Regional Office
3190 160th Ave., SE
Bellevue WA 98008-5452
Ph: (206) 649-7257

May, 1994

TABLE OF CONTENTS

1.0 INTRODUCTION	
1.1 Background	1
1.2 Objectives	2
1.3 Field Methods	2
1.4 Grain Size Analyses	3
2.0 THEORY	
2.1 Interpretation of the X-Distribution	4
2.2 Interpretation of a trend	5
3.0 PHYSICAL SETTING	
3.1 Geology and Physiography	7
3.2 Tides, Currents and Winds	8
3.3 Anthropogenic Disturbances	8
4.0 PATTERNS OF SEDIMENT TRANSPORT	
4.1 Mud Transport	10
4.2 Sand Transport	13
5.0 DISCUSSION	
5.1 General Considerations	15
5.2 Implications for Dredging Activities	18
5.3 Implications for Contaminant Transport	19
5.3.1 Introduction	19
5.3.2 Correlation between sediment transport and heavy metals	20
5.3.3 Sites for Environmental Monitoring	22
6.0 SUMMARY AND CONCLUSION	24
7.0 ACKNOWLEDGMENTS	27
8.0 REFERENCES	28

APPENDIX I: Sediment Transport Model

LIST OF FIGURES

- Figure 1: Sample location map and place names used in the text
- Figure 2: Sediment types in Elliott Bay and the Duwamish River
A: Sand and muddy sand
B: Mud and sandy mud
C: Mud
- Figure 3: Areas of anthropogenic disturbances in Elliott Bay (Information from P. Romberg, Metro; pers. comm. 1993) (See Table 1)
- Figure 4: Sample lines used to determine net sediment transport for mud.
- Figure 5: Net sediment transport pathways for mud
- Figure 6: D₁, D₂ and X for Line 11m
- Figure 7: D₁, D₂ and X for Line 18m
- Figure 8: D₁, D₂ and X for Line 23m
- Figure 9: D₁, D₂ and X for Line 29m
- Figure 10: D₁, D₂ and X for Line 34m
- Figure 11: D₁, D₂ and X for Line 39m
- Figure 12: D₁, D₂ and X for Line 40m
- Figure 13: D₁, D₂ and X for Line 51m
- Figure 14: D₁, D₂ and X for Line 76m
- Figure 15: Sample lines used to determine net sediment transport for sand
- Figure 16: Net sediment transport pathways for sand.
- Figure 17: D₁, D₂ and X for Line 1s
- Figure 18: D₁, D₂ and X for Line 3s
- Figure 19: Sample locations for heavy metal concentrations (EPA, 1993). Lines A and B follow the transport pathways defined by Lines 24 and 34 respectively (Fig. 4)
- Figure 20: Heavy metal concentrations with distance - East Waterway
- Figure 21: Heavy metal concentrations with distance - West Waterway
- Figure 22: Recommended environmental monitoring sites

LIST OF TABLES

- Table 1: Partial list of areas of anthropogenic disturbances (see Figure 3)
- Table 2A: Sediment trend statistics for all lines of mud samples
- Table 2B: Sediment trend statistics for all lines of sand samples.
- Table 3A: Summary of the sediment transport environments contained in Elliott Bay and the Duwamish River (mud)
- Table 3B: Summary of the sediment transport environments contained in Elliott Bay and the Duwamish River (sand)

1.0 INTRODUCTION

1.1 Background

Seattle and its associated industry are concentrated on the Elliott Bay waterfront and the Duwamish River (Fig. 1). As a result these waters have a long history of anthropogenic disturbances that date from the turn of the century. These include dredging for dock construction, dredged material disposal, significant contaminant inputs, and sediment capping operations designed to stabilize contaminated sediments.

A fundamental requirement for rational estuarine management is to assess the stability of contaminated sediments, as well as to determine the long-term fate of dumped materials. Such an understanding is inextricably linked with the behavior of natural sediments and their relationship with anthropogenic inputs and/or disturbances. In particular, net sediment transport directions must be known, together with the dynamic behavior of the environment (i.e. erosion, deposition, equilibrium etc.). Unfortunately, sediment transport is generally difficult to model, particularly in the case of estuaries, for a variety of reasons. Water movements are tidally dependent, changing in their direction, intensity and duration; also small errors in grain-size characteristics, bathymetry, bed type and bed friction can create significant errors in the solution (Black and Barnett, 1988). Often, natural erosion or deposition rates are too slow for bed changes to be measured for comparison with model predictions. Thus, any method that can help to calibrate the results of a transport model would greatly enhance its reliability as a predictive technique.

The principal aim of this report, therefore, is to establish the net transport patterns using a relatively new technique known as a Sediment Trend Analysis. First described in McLaren and Bowles, 1985, this approach uses for its data, relative changes in complete grain-size distributions of the existing sediments. The derived patterns of transport are, in effect, an integration of all processes responsible for the erosion, transport and deposition of sediments over the time period required to form the deposits. In addition, the analysis provides information on the probability of each grain-size being transported which directly relates to the dynamic behavior of the sedimentological environment.

Although this approach is largely qualitative (it is unable to establish rates of transport or deposition), the results have been particularly useful in a large variety of studies to: (1) evaluate and direct numerical models (Van Heuvel, et al., 1993; McLaren, Collins et al., 1993); (2) determine the behavior of sediments at dredged material disposal sites (McLaren and

Powys, 1989); (3) predict the build-up and dispersal of contaminated sediments (McLaren, Cretney et al , 1993; Little and McLaren, 1989); and (4) understand the sediment and process interrelationships among natural marine and coastal environments (De Meyer and Wartel, 1988).

1.2 Objectives

The specific objectives of this project were to:

- (1) collect about 500 sediment grab samples from Elliott Bay and the Duwamish River (Fig 1);
- (2) analyze each of the samples for their complete grain-size distributions and to establish, using the technique of sediment trends, the present patterns of sediment transport;
- (3) determine areas of erosion, stability (dynamic equilibrium) and deposition;
- (4) correlate the derived patterns of transport with known processes;
- (5) use the above findings in order to:
 - (i) assess the stability of existing dumpsites;
 - (ii) determine the probable dispersal and/or accumulation of contaminants contained in the sediments;
 - (iii) advise on the locations of future environmental monitoring programs;
 - (iv) suggest, if applicable, possible solutions to mitigate the environmental consequences associated with existing estuarine management programs.

1.3 Field Methods

To provide an adequate sample density, taking into consideration the variety of anthropogenic disturbances to the sediments in Elliott Bay, and in particular along the waterfront, a sampling strategy was designed on three separate grid spacings. Samples were separated at 10 seconds of latitude intervals (310 m) in outer Elliott Bay (from the west end of the study area to a line extending from Duwamish Head to Smith Cove, Fig 1). In inner Elliott Bay spacing was reduced to 8 second intervals (250 m) and a still smaller interval (150 m) was used in the Duwamish Waterway (both

East and West Waterways and the river as far south as the "Turning Basin"). Additional samples were collected, regardless of the designed sample grid, near the shoreline and between piers along the waterfront.

Field work was carried out between Oct 4 and Oct 17, 1993, using a temporarily converted fishing vessel, BRENDON "D" II. This was equipped with a Global Positioning System (GPS), and a hydraulic winch and boom that allowed for the operation of a Shipek Grab Sampler. This device enabled the top 10 to 15 cm of sediment to be sampled and worked extremely well. At 30 locations specified by the client (Fig. 1), a second grab sample was collected to establish sample similarity and to compare the sediment trends with both the original and duplicate samples.

Representative samples from the grab were stored in plastic bags and shipped to the GeoSea office in Cambridge, U.K. for grain size analyses. In all a total of 568 samples were collected.

1.4 Grain Size Analyses

The samples were all analyzed using a standardized method developed by GeoSea Consulting. This combines measurements on a Malvern 2600L laser particle sizer with data obtained from dry sieving the gravel and coarse sand fractions (-2.0 phi to -0.5 phi) where necessary. All samples, including 30 duplicate samples, were well mixed prior to analysis in order to obtain a representative sub-sample.

The Malvern instrument employs lenses of different focal lengths to look at portions of the total range of grain sizes. Frequently, two measurements were required; one to encompass the sand fraction and the other the silts and clays. The separate distributions and sieve data were then "merged" together using an algorithm developed by GeoSea to re-proportion the weight per cents into a single, complete distribution. The merged distributions provide the data base used in the sediment trend analysis. A copy of the data base, including a disk file, was previously submitted to the client (GeoSea Consulting (Canada) Ltd., 1993).

2.0 THEORY

The technique to determine the sediment transport regime utilizes the relative changes in grain-size distributions of the bottom sediments. The derived patterns of transport are, in effect, an integration of all processes responsible for the transport and deposition of bottom sediments over the period of time represented by the actual samples. Details of the theory are described in Appendix I; however, the approach is summarized here.

Suppose two sediment samples (D_1 and D_2) are taken sequentially in a known transport direction (for example from a river bed where D_1 is the up-current sample and D_2 is the down-current sample). The theory shows that the sediment distribution of D_2 may become finer (Case B) or coarser (Case C) than D_1 ; if it becomes finer, the skewness of the distribution must become more negative. Conversely, if D_2 is coarser than D_1 , the skewness must become more positive. The sorting will become better (i.e. the value for variance will become less) for both Case B and C. If either of these two trends is observed, we can infer that sediment transport is occurring from D_1 to D_2 . If the trend is different from the two acceptable trends (e.g. if D_2 is finer, better sorted and more positively skewed than D_1), the trend is unacceptable and we cannot suppose that transport between the two samples has taken place.

In the above example, where we are already sure of the transport direction, $D_2(s)$ can be related to $D_1(s)$ by a function $X(s)$ where 's' is the grain size. The distribution of $X(s)$ may be determined by:

$$X(s) = D_2(s)/D_1(s)$$

$X(s)$ provides the statistical relationship between the two deposits and its distribution defines the relative probability of each particular grain size being eroded, transported and deposited from D_1 to D_2 .

2.1 Interpretation of the X-Distribution

Empirical examination of X-distributions from a large number of different environments has shown that four basic shapes are most common when compared to the D_1 and D_2 distributions (Fig A-5; Appendix I). These are as follows:

(1) Dynamic Equilibrium: The shape of the X-distribution closely resembles the D_1 and D_2 distributions. The relative probability of grains being transported, therefore, is a similar distribution to the actual deposits. This

o

suggests that the probability of finding a particular grain in the deposit is equal to the probability of its transport and redeposition (i.e. there is a grain by grain replacement along the transport path). The bed is neither accreting nor eroding and is, therefore, in dynamic equilibrium.

(2) Net Accretion: The shapes of the three distributions are similar, but the mode of X is finer than the modes of D₁ and D₂. Sediment must fine in the direction of transport; however, more fine grains are deposited along the transport path than are eroded, with the result that the bed, though mobile, is accreting.

(3) Net Erosion: Again the shapes of the three distributions are similar, but the mode of X is coarser than the D₁ and D₂ modes. Sediment coarsens along the transport path, more grains are eroded than deposited, and the bed is undergoing net erosion.

(4) Total Deposition: Regardless of the shapes of D₁ and D₂, the X-distribution more or less increases monotonically over the complete size range of the deposits. Sediment must fine in the direction of transport; however, the bed is no longer mobile. Rather, it is accreting under a "rain" of sediment that fines with distance from source. Once deposited, there is no further transport.

Recently, a fifth form of the X-distribution (not described in Appendix I) has been discovered. Occurring only in extremely fine sediments when the mean grain-size is very fine silt or clay, the X-distribution may be essentially horizontal. Such sediments are usually found far from their source and the horizontal nature of the X-distribution suggests that their deposition is no longer related strictly to size-sorting. In other words, there is now an equal probability of all sizes being deposited. This form of the X-distribution was first observed in the muddy deposits of a British Columbia fjord and is described in McLaren, Cretney et al., 1993.

2.2 Interpretation of a Trend

In reality, a perfect sequence of progressive changes in grain-size distributions are seldom observed in a line of samples, even when the transport direction is clearly known. This is due to complicating factors such as variation in the grain-size distributions of source material, local and temporal variability in the X(s) function, and a variety of sediment sampling difficulties (i.e. sample doesn't adequately describe the deposit; its taken too deeply; not deep enough etc.)

Initially, a trend is easily determined using a statistical approach whereby, instead of searching for "perfect" changes in a sample sequence, all possible pairs contained in the sequence are assessed for possible transport

direction. When one of the trends exceeds random probability within the sample sequence, we infer the direction of transport and calculate $X(s)$. The precise statistical technique is described more fully in Appendix I.

Despite the initial use of a statistical test, various other qualitative assessments must be made in the final acceptance or rejection of a trend. Included is an evaluation of R^2 , a multiple correlation coefficient defining the relationship among the mean, sorting and skewness in the sample sequence. If a given sample sequence follows a transport path perfectly, R^2 will approach 1.0 (i.e. the sediments are perfectly "transport-related"). A low R^2 may occur, even when a trend is statistically acceptable for the following reasons: (i) sediments on a presumed transport path are, in reality, from different facies, and valid trend statistics occurred accidentally; (ii) the sediments are from a single facies, but the chosen sequence is only a poor approximation of the actual transport path, and (iii) extraneous sediments have been introduced into the natural transport regime, as in the case of dredged material disposal. R^2 , therefore, is assessed qualitatively, and when low, statistically accepted trends must be treated with caution.

To analyze for sediment transport directions over 2-dimensions, a grid of samples is required. Each sample is analyzed for its complete grain-size distribution and these are entered into a micro-computer equipped with appropriate software to calculate statistically acceptable trends for all sample sequences and the corresponding transport ($X(s)$) functions. Most importantly, a final interpretation of the sediment pathways is accepted only when the patterns of transport form a "coherent whole" over the entire area of sampling.

3.0 PHYSICAL SETTING

3.1 Geology and Physiography

The whole of Puget Sound is contained by a shoreline composed principally of poorly sorted glacial deposits (Downing, 1983). These are commonly exposed in the numerous eroding bluffs common to the region, although coastal works have been widely used to decrease the rate of erosion (e.g. Magnolia Bluff; Fig. 1). As a result of a more or less ubiquitous sediment source at the shoreline, erosion and sediment transport has nearly everywhere produced a sedimentary sequence of nearshore sands and gravels that grade into muddy sands, sandy muds and finally mud in the deeper water (see, for example, regional maps produced by Roberts, 1979)

In Elliott Bay itself, despite considerable anthropogenic disturbances, this same sequence of sediment types can be clearly differentiated (Fig. 2). Sandy deposits are confined to depths more or less shallower than 300 feet (91 m), below which mud dominates. Only along the Seattle waterfront where mud continues from the deep water all the way to the shoreline is this sequence disturbed (Fig. 2C). Mud and sandy mud also dominate the Duwamish River and both the East and West Waterways.

The bathymetry of Elliott Bay is characterized by a central submarine canyon that originates from two tributaries trending north-south and northwest-southeast. The latter are probably erosional features carved into underlying glacial deposits by an early Holocene "Duwamish River" when sea-levels were lower and flows very much higher than today.

Blomberg et al., 1988, estimated that Duwamish River discharge in the mid-1800's (i.e. before significant anthropogenic disturbance) ranged from 2500 cfs to 9000 cfs ($68 \text{ m}^3 \text{ s}^{-1}$ to $243 \text{ m}^3 \text{ s}^{-1}$). At that time, the lower 6 miles of the river was contained within a tidal marsh that opened onto a broad expanse of intertidal flats through which there were three main distributary channels. Today, discharge varies from about $12 \text{ m}^3 \text{ s}^{-1}$ in August to $83 \text{ m}^3 \text{ s}^{-1}$ in January (Baker et al., 1983) with an average of $50 \text{ m}^3 \text{ s}^{-1}$ (EPA, 1988a). According to EPA (1993), about 80 per cent of the sediment load contained in the river is deposited in the lower reaches affected by the salt-wedge. Suspended sediments are carried at times of peak flows into Elliott Bay where they are contained in a buoyant surface plume (2 m in depth) (Paulson et al., 1989). The latter tends to travel in a counterclockwise direction along the eastern shore of Elliott Bay and then westwards along the northern shoreline (Curl et al., 1988; Sillcox et al., 1981)

3.2 Tides, Currents and Winds

Tides in Elliott Bay are normally semi-diurnal with a maximum range of about 13 feet (3.9 m). The flood enters Puget Sound from the north and tends to generate clockwise currents inside Elliott Bay. On the ebb, however, current patterns are not exactly reversed (i.e. counterclockwise); rather the Bay becomes influenced by the formation of several smaller gyres, some clockwise while others are counterclockwise (McGary and Lincoln, 1977). Both surface and deep currents within the bay tend to be weak, the mean velocity being typically less than 0.2 fps (Cox et al., 1981).

In the Duwamish River, a tidally-driven saltwater wedge is overlain by freshwater moving downstream. During periods of low flow, the wedge has been detected as far as 10 miles upstream. With river flows exceeding 1000 cfs ($28 \text{ m}^3 \text{ s}^{-1}$), the wedge is maintained about 8 miles upstream (about 2 miles upriver of the Turning Basin) regardless of the tidal stage. Currents in West Waterway range from 1.4 fps near the surface to 0.2 fps near the bottom (EPA, 1993).

Wind direction is largely controlled by the topography surrounding Puget Sound. Summer winds are most often light and from the north whereas in winter they are much stronger and blow from the south and southwest. The latter are clearly dominant with respect to longshore sediment transport and numerous northward-trending spits are prevalent in the southern Sound (Downing, 1983). Because fetches are generally limited, in Elliott Bay wave periods are typically less than 2 ft (0.6 m) with periods of 2 to 2.5 s. These heights can easily be doubled by the action of vessel swash.

3.3 Anthropogenic Disturbances

The coasts of Elliott Bay and the Duwamish River have been more or less under continuous anthropogenic modification since the beginnings of urbanization. In the Duwamish River, the lower 6 miles of the once-meandering river is now a straightened navigation channel that is maintained by the U.S. Army Corps of Engineers as far as the Turning Basin (Fig. 1). Here sediments have been removed to provide capping material for contaminated sites along the Seattle waterfront. At the river mouth, the former large expanses of mudflats are covered by industrial complexes and the river's course is controlled by the dredged channels making up the East and West Waterways. Harbor Island itself was constructed primarily from dredged materials.

Figure 3 provides a summary of the principal anthropogenic disturbances effecting Elliott Bay (see also Table 1), some of which are clearly visible in the sediment-type maps (Figs. 2A, 2B, and 2C). For example, the PSDDA disposal site (#4 in Fig. 3) is delineated in Figures 2A and 2B. Region 12 (Fig. 3) is also highlighted in Figures 2A and 2B, an area that has received considerable amounts of sand as a result of sandblasting operations (T Michelsen, 1993; pers. comm.). An area of coarse sediments is visible slightly seaward of the Seattle waterfront (Fig. 2C) which appears to correlate with the huge amounts of sediments that were dumped during the "Denny regrade" construction (#1, Table 1, and Fig. 3). Unfortunately in this study, only the extreme eastern edge of the Four Mile Rock disposal site was sampled (Figs. 1 and 3) and its "signature" was not apparent.

Considerable research has taken place on the sources and fate of the large amounts of contaminants that enter the Duwamish River and Elliott Bay (e.g. Curl et al., 1988; EPA, 1988a, 1988b). It is recognized that contaminant levels are unacceptably high in many of the sediments, particularly along the Seattle waterfront, and major efforts are presently underway to determine remedial action. According to Curl et al., (1988), the highest concentrations of toxicants originate from the West Duwamish Waterway, the North End of Harbor Island, the Denny Way combined sewer overflow (CSO) and the Seattle waterfront.

4.0 PATTERNS OF SEDIMENT TRANSPORT

Of the 533 samples collected in Elliott Bay and the Duwamish River (not including duplicates), the sediments fell into the following types:

- (1) gravel - 0%
- (2) sandy gravel - 1%
- (3) gravelly sand - 1%
- (4) sand - 11 %
- (5) muddy sand - 15%
- (6) sandy mud - 20%
- (7) mud - 51%

Because previous studies have shown that different sediments (i.e. facies) may behave differently from each other, considerable effort was made to establish separate transport patterns for each type. In particular, mud which is usually a cohesive sediment may follow different transport paths from non-cohesive sand, and bimodal distributions often behave according to the proportion of mud present in the distribution (i.e. usually sand with more than 20% mud content will behave as a cohesive sediment). In this study, however, good trends were established for mud and sandy mud as one sediment type, and for sand and muddy sand as a second sediment type. These will be referred to as the mud and sand facies respectively. As part of the quality control, identical trends were undertaken using, where required, the duplicate samples. For each line of samples where one or more samples have been substituted by a duplicate, the trend statistics are included in Table 2

4.1 Mud Transport

Following the calculation of numerous sample sequences to determine significant trends, a total of 81 lines were selected to provide a pattern of transport that appeared to be consistent over the whole area. These sample lines are shown in Figure 4 and the individual trend statistics are contained in Table 2A. Figure 5 illustrates the net sediment transport pathways. The findings are summarized as follows:

(1) Seattle Waterfront - Lines 1 to 26

These lines originate immediately adjacent to Piers 90 and 91 on the north side of Elliott Bay. They follow the very nearshore mud deposits found along the waterfront and most of the lines terminate inside individual docks. Lines 23 to 25, however, terminate at the south end of East Waterway. The R^2 values are not particularly high ($R^2=0.810.10$) and show a wide range of values (Tables 2A and 3A), probably the result of the high degree of anthropogenic disturbance that is present along the docks (Fig. 3).

This may also account for the difficulty in achieving a clearly defined X-distribution. It might be expected to find an X-distribution indicative of total deposition occurring inside the sediment traps created by the docks (see Fig. A-5; Appendix I). In fact, the distribution tends to change from north to south along the waterfront. In the first 17 lines, the principal mode of X generally falls inside the modes of the D₁ and D₂ distributions, a feature indicative of dynamic equilibrium (Fig. 6). However, the tail of the X-distribution is atypical, and shows a secondary fine mode outside the D₁ and D₂ distributions suggesting net accretion. Possibly the coarse portion of the sediments in transport are in dynamic equilibrium, whereas there is slight accretion occurring in the fines.

In the lines farther south (Lines 18 to 22), most of the X-distributions become nearly horizontal over the fine portion of the D₁ and D₂ distributions, a feature suggesting that the importance of size-sorting is decreased with distance from the original source (Fig. 7). In East Waterway itself, the X-distributions, although nearly horizontal, actually monotonically increase throughout the range of the D₁ and D₂ distributions indicating total deposition in this area (Fig. 8).

(2) Seattle Nearshore - Lines 27 to 32

These lines parallel both the Seattle Waterfront lines and the natural bathymetry of Elliott Bay down to a depth of about 300 feet (91 m). The trends show a clearly defined transport regime directed southeast along the waterfront with a clockwise component that terminates in the vicinity of the PSDDA disposal site. The R^2 values are generally higher than the lines immediately adjacent to the Seattle Waterfront ($R^2=0.870.08$; Table 3A), possibly reflecting a decrease in anthropogenic disturbance. Most of the X-distributions show a shape indicating net accretion along the transport path, although again the fine mode is only poorly defined (Fig. 9).

(3) Harbor Island - Lines 33 to 42

These lines originate between Terminal No. 46 and the PSDDA disposal site. They are very similar to the Seattle Waterfront lines in that they follow the shoreline and terminate inside the finger docks. The R^2 values, although somewhat higher than those for the Seattle Waterfront ($R^2=0.860.17$; Table 3A) have a larger standard deviation (i.e. there is a greater spread of values). Once again, the X-distributions are poorly defined. Inside West Waterway (Lines 33 to 35), they appear to show slight net accretion, although the mode is not very "peaked" (Fig. 10). In two of the lines (36 and 39) which are terminated inside finger docks, the X-distribution is more or less monotonically increasing indicating total deposition (Fig. 11). Finally, there is even evidence for dynamic equilibrium (Lines 37 and 40; Fig. 12).

(4) Central Elliott Bay - Lines 43 to 74

Like the Harbor Island lines, this large group of lines originates south and east of the PSDDA disposal site. They continue the clockwise transport direction around the circumference of the Bay, paralleling the shoreline past Duwamish Head, and radiating west and north into outer Elliott Bay. Inside the Bay, the transport continues to be clockwise with many lines terminating against the Seattle Nearshore regime. The gyre becomes increasingly "tight" with the last few lines ending inside the northeast canyon. Compared with all the previous environments, the R^2 values are relatively high and constant ($R^2=0.890.05$; Table 3A) suggesting that anthropogenic disturbances decrease with distance from the shoreline. Nearly all the X-distributions show slight net accretion, although for those lines that are principally below 300 feet, the distribution becomes increasingly horizontal (Fig. 13).

(5) Georgetown Reach - Lines 75 to 78

This group of lines originates near Slip 2 on the Duwamish River. Sediment transport is directed downstream to the junction between the East Waterway and Harbor Island Reach. The trend statistics are excellent with $R^2=0.880.01$. The X-distributions nearly all show the case of total deposition (Fig. 14).

(6) Upper Duwamish River - Lines 79 to 81

Originating near Slip 3 in the Duwamish River, these lines suggest that transport is occurring in an upstream direction to the Turning Basin. The R^2 values are relatively low ($R^2=0.800.13$; Table 3A) and the X-distributions were, in general, difficult to interpret. For these reasons, the transport trends in this region should not be considered very reliable.

4.2 Sand Transport

Compared with the number of mud samples (392) there are far fewer sand samples (138) and consequently fewer trends. A total of 29 lines of samples (Table 2B) were determined and these are grouped into 5 transport environments (Table 3B). Sample lines and the corresponding transport pathways are shown in Figs. 15 and 16 respectively.

(1) Magnolia Bluff - Lines 1 to 7, 19

These lines are comprised of the sand samples adjacent to Magnolia Bluff. Trends were obtained by using the sand portion of the distribution only (mud contents are generally quite small in this area). The trend statistics are relatively low and variable ($R^2=0.850.14$; Table 3B) which may be due to an increasing mud content towards the Seattle Waterfront. The line closest to the shore (Line 1) provides an X-distribution indicative of net erosion (Fig. 17); the remaining lines appear to be in dynamic equilibrium (Fig. 18).

(2) Harbor Island (Lines 8 to 18)

Originating in the Magnolia Bluff group of lines, these sample sequences follow the Seattle Waterfront and terminate in the finger docks of Harbor Island and Pier 4. The samples are principally bimodal with mud contents 20% and 50%. The statistics of the lines are excellent ($R^2=0.960.01$; Table 3B); however, the trends were obtained for both Case B and Case C transport and there was no clear interpretation for the X-distribution. Of the two Cases, a coarsening sequence (Case C) is dominant (Table 2), possibly caused by the anthropogenic sand associated with the north shore of Harbor Island (Fig. 3).

(3) Duwamish Head - Lines 20 to 26

These lines parallel the shoreline from an area west of Pier 4 into outer Elliott Bay. Mud contents are generally too low to be included in the distributions. Similar to the Magnolia Bluff lines, these trends display a mixture of erosion and dynamic equilibrium (Table 2). R^2 values are reasonably high ($R^2=0.920.04$).

(4) PSDDA Disposal Site - Lines 27 and 28

Using the only sand samples available on the PSDDA disposal site, 2 lines of three samples each were obtained. Ordinarily, trends on such a small number of samples would not be discussed; however, they are reported here simply because the derived transport paths conform to the clockwise gyre already determined in the sediment trend analysis for mud. The derived trends are not, however, consistent. One line indicates net accretion whereas the other appears to show net erosion.

(5) Harbor Island Reach - Line 29

This single line of samples indicates upriver transport of sand through the narrow channel connecting West Waterway with the Duwamish River.

5.0 DISCUSSION

5.1 General Considerations

The transport patterns for mud and sand as shown in Figures 5 and 16 represent an interpretation of the net sediment movement occurring in Elliott Bay and the Duwamish River. It is important to emphasize that the patterns have been developed without regard to the possible processes that may be responsible; rather the pathways have been "discovered" purely on the basis of statistically acceptable changes in the grain-size distributions of the sediments themselves.

The most dominant characteristic of the transport regime in Elliott Bay is the presence of a well-defined clockwise gyre. The fact that the trends determined for both the mud and sand sediment types are essentially similar provides considerable support for their validity. Nevertheless, the clockwise gyre is, perhaps, a surprising finding given that the sediment plume associated with the Duwamish River is known to travel counterclockwise along the Seattle Waterfront (Curl et al., 1988).

In fact, early modeling studies by Rogers (1955) and Winter (1977) postulated a clockwise circulation in Elliott Bay. Current measurements taken in later studies, however, tended to contradict this model and several syntheses of net current velocities display a rather confused variety of different patterns, few of which agree with each other, but none specifically supporting the presence of a clockwise gyre (e.g. Silcox et al., 1981; URS Engineers and Evans-Hamilton, 1986).

It is generally agreed that currents in Elliott Bay are, for the most part, insufficient to cause resuspension and further transport of sediment (Curl et al., 1988). For this reason it can, perhaps, be expected that a single vector representing mean current velocity does not provide any indication of the direction of net sediment transport. However, despite considerable variety in the shapes of the X-distributions, it appears clear that some transport is occurring in water depths less than 300 feet. Below 300 feet, X-distributions are essentially horizontal indicating a "rain" of particles that are no longer size-differentiated. Therefore, a process must exist to achieve the derived patterns.

The transport pathways in Elliott Bay suggest that the Duwamish River is not responsible for the ultimate directions of transport. Rather, it serves to supply particulate matter in its plume which is carried along the Seattle Waterfront. On settling through the pycnocline, these particles are inextricably mixed with sediments from shoreline sources and are

transported and deposited in the reverse direction. It is already realized that the surface plume supplies only a minor fraction of the sediment accumulating on the floor of the bay, and that the shoreline is probably the most important contributor to sedimentation. This observation was made by Baker et al , (1983), and the findings of the present study certainly concurs.

The presence of the Duwamish River and its associated plume are undoubtedly responsible for the mud deposits that are shallower than 300 feet in the region adjacent to the Seattle Waterfront (Fig. 2C). It is not, however, responsible for the direction of net sediment transport. Elsewhere, in both Elliott Bay and Puget Sound as a whole, typical sedimentological sequences reflect glacial sediments as a source at the shoreline which are reworked and transported by littoral processes to produce a "classic" sequence of fining sediments towards the offshore. A shoreline, for it to be an effective source, must erode and this generally occurs with extreme events. Such events are most likely to happen in winter when south and southwest winds are strongest. Furthermore, wind driven currents from these directions would favour the development of a clockwise gyre in Elliott Bay. Possibly a detailed analysis of tidal residuals, or strength and duration of bottom currents in association with extreme storm events might demonstrate the probability of currents capable of resuspension and deposition in water depths above 300 feet.

There is much evidence to suggest that the amount of natural sediment available for deposition is very small. Peak flows for the Duwamish River are about one third that of the pre-industrialized river. Throughout Puget Sound in general, the amount of shoreline available for erosion is constantly being decreased. The sediment types defined for this study appear to delineate fairly accurately areas of anthropogenic disturbance; vigorous transport processes or high deposition rates would rapidly cause their "signatures" to be lost. The large variety of X-distributions together with difficulties encountered in providing a clear interpretation are attributed to the high degree of anthropogenic disturbance of the natural sediments. Again, a greater supply of natural sediments coupled with stronger processes would undoubtedly lessen such ambiguities.

The paucity of natural sediments may be reflected in West Waterway. Despite the transport trends that suggest there should be net accretion, recent bathymetric surveys show either stability or net erosion in the long-term (about 10 years) (Roy F. Weston, Inc., in press). This is an important finding and may well provide an understanding of the nature and timing of processes that must be considered. Extreme events acting on the shoreline in outer Elliott Bay suspend and transport sediments into West Waterway; however, extreme events associated with the Duwamish River must be capable of flushing these deposits back into the Bay. Flushing is evidently not as effective in East Waterway where there appears to be total deposition of fine grained sediments.

There may well be an anthropogenic process to consider along the Seattle Waterfront where ship's propeller wash may aid in maintaining erosion and transport of fine sediments that are deposited inside the finger docks. Such docks are typically sediment traps and total deposition is ordinarily expected; however, the X-distributions show only slight net accretion suggesting that sediment transport is occurring both in and out of the individual docks.

Evidence to support the dominance of the clockwise transport gyre in Elliott Bay is rare. Most studies have been concerned with the importance of the Duwamish River plume and there are a variety of contour maps showing the concentrations of suspended particulate matter and associated contaminants both at the surface and near the bottom. Generally, the contours have been constructed to emphasize an apparent dispersal in the direction of the plume (e.g. Baker, 1982). However, it is possible to view the values as increasing in the direction of net sediment transport, particularly for those taken near the bottom. In one particular study (Curl, 1982), a sequence of contour maps for a variety of contaminants in both surface and bottom waters follow with considerable accuracy the derived patterns of transport. It has also been observed in these studies that high concentrations of particulate matter and heavy metals are frequently found on the bottom of the northeast canyon, a location marking the end of the transport paths for the Elliott Bay gyre.

Some physical evidence for the Magnolia Bluff transport regime (Table 3B) is an observation of bedforms offshore from Smith Cove. Here, sonograms showed bottom current-generated bedforms oriented into Elliott Bay (Cooper Consultants, 1986). Unfortunately water depths are not provided, but their location shown on a sketch map (without a scale) suggests that the sediments are mobile in about 200 feet of water. This same report also describes bedforms on the PSDDA disposal site located about 0.75 nm north of Harbor Island in over 220 feet of water. Their orientation was not reported; however, their presence confirms the mobility of sand at these depths.

The transport pathways in the Duwamish River are also surprising. Upriver transport was determined in both East and West Waterways and in the upper reaches of the river as far as the turning basin. Downriver transport was determined only in the Georgetown Reach. Because these trends are dependent more or less on a single line of samples, they should be regarded with caution. Nevertheless, there is a clear indication that the flood tide dominates deposition in this portion of the river rather than the river itself. Undoubtedly the Duwamish River does supply sediments, but from the trend analysis, it is clear that for silt and clay, they are incorporated in the flood-dominated system and may not easily "escape" from the estuary.

5.2 Implications for Dredging Activities

According to D. Kendall (U.S Corps Dredge Material Management Office, pers. comm) dredging in the Duwamish River is routinely undertaken about every two years and disposed of in the PSDDA disposal site. At the Turning Basin, clean sands have been removed to cap contaminated sediments along the Seattle Waterfront (Sumeri and Romberg, 1991). If the transport trends for mud (Fig.5) are correct, the origin of the deposits in the Duwamish is quite complex. (The anomalous seaward direction of sediment transport in Georgetown Reach is, for the moment, being ignored.) Fine material is carried by the river, first in the fresh water plume and into Elliott Bay, before returning as a near-bottom load contained in the salt wedge. The return sediments undoubtedly contain a mixture of river and Elliott Bay sediments.

Flood-directed sedimentation of mud in estuaries is quite common and is usually the result of asymmetric tidal currents where the flood is faster flowing and of shorter duration than the ebb. Fine sediments are carried in suspension on the flood with deposition occurring at high water slack. Given the cohesive nature of mud, the weaker ebb regime is unable to resuspend and return the sediments as easily as the stronger flood currents. In this way, there is a continual "tidal pumping" of mud in the landward direction. Sand, on the other hand, is non-cohesive and, despite a weaker ebb current, can be returned towards the sea. Because the duration of the ebb is longer than the flood, the net effect will be to transport sand, if it is present, down-river.

Model experiments in Germany that were confirmed in a recent GeoSea study have shown how the effects of channel deepening actually increases tidal range which, in turn, serves to force more sediment upstream (Jenson and Sieffert, 1994). In the Duwamish River, the amount of sediment is clearly not large; however, the sediment trends provide at least some evidence that such tidal forcing is indeed taking place. It should also be noted that the sampling program undertaken for this study revealed very little sand actually in the Duwamish River; even at the Turning Basin most of the samples were muddy (Figs.2B and 2C). It is possible that the Duwamish River is no longer transporting the sand loads that it may have been capable of in the past, in which case sand removal at the Turning Basin may be encouraging mud deposition from farther downstream. This may be particularly undesirable since these muds will have the potential of being significantly contaminated.

The above remarks are both speculative and cautionary. The mud trends in the Upper Duwamish to the Turning Basin were rather poor, and the X-distributions were not clear. Furthermore, the down-river trends in

Georgetown Reach were much more acceptable. The latter may only be a local phenomenon in the overall hydrodynamics of the river caused by the complexities of the confluence of the two Waterways as well as artificial deepening to form a turning basin in this area of the river. There is clearly a requirement for further work to ascertain the effects of dredging on sediment transport in the Duwamish River.

In Elliott Bay where material is dumped at the PSDDA disposal site and coarse sediments are used to cap areas of the Seattle Waterfront, the sediment trends do suggest that transport off the sites is possible. In general, the sand trends show dynamic equilibrium indicating that at present there is transport without erosion or deposition. The presence of bedforms near the Four Mile Rock site and the PSDDA site attests to the possibility of sediment movement in water depths well below 200 feet (Cooper Consultant's Inc., 1986). Another indication of sediment transport from anthropogenic sources is seen in Figure 2C that shows sediments in West Waterway are generally sandier than in East Waterway. Given that the transport pathways into West Waterway pass over the ship yard sand deposits (#12, Fig 3) as well as passing close to the PSDDA disposal site, there is more opportunity for sand to enter the West Waterway compared to the East Waterway.

Despite the above observations, the anthropogenic sites appear well defined by their sediment signatures which is, in part, the result of very slow deposition rates of natural sediments (i.e. the rate of coverage is slow), as well as very small transportation rates of the coarser sediments. The sediment trend analysis does indicate, however, that any disposal of material shallower than 300 feet does have some probability of further movement off the site. At depths greater than 300 feet, any movement appears unlikely and disposed material would become eventually buried by a "rain" of suspended sediments.

5.3 Implications for Contaminant Transport

5.3.1 Introduction

The relationships between contaminants and sediment transport pathways were first determined in a study by McLaren and Little (1987). Similar findings have been observed in a variety of environments, including Liverpool Bay and the Bristol Channel in the U.K., Sullom Voe in the Shetland Islands, and in Howe Sound on the west coast of Canada (McLaren, Cretney, et al., 1993). These may be summarized as follows:

- (1) Given a greater surface area and more sites available for adsorption, contaminants have a greater association with fine sediment (silt and clay) than with coarse sediment (sand).
- (2) Sediments in dynamic equilibrium (Fig. A-5,A; Appendix I) show no relationship between contaminant loadings and distance along the transport path.
- (3) In environments undergoing net accretion (Fig. A-5,B; Appendix I) there is a general linear increase of contaminant loading along the transport path. Because sediment transport is the cause of concentrating contaminants in the environment, the specific relationship between contaminants and their sources can be lost.
- (4) Contaminant loadings decrease rapidly along an eroding transport path (Fig. A-5,C; Appendix I).
- (5) In environments of total deposition (Fig. A-5,D; Appendix I), contaminants are found as localized "highs" that can generally be associated with a specific source.
- (6) When the X-distribution is horizontal, all particles, whether contaminated or not, have an equal probability of deposition. There is not, therefore, any preferred area for the deposition of contaminants and more or less constant concentrations are to be expected throughout such an environment.

5.3.2 Correlation between sediment transport and heavy metals

Considerable contaminant data for sediments along the Seattle Waterfront and in the Duwamish River are reported in Roy F. Weston, Inc., (in press). Unfortunately, most of the sample locations were selected as close as possible to known sources of contaminants (e.g. immediately adjacent to the Seattle Waterfront, inside finger docks, and close to outfalls). In this case, the sampling program followed a common tendency to monitor sediments as close as possible to known contaminant sources. Although this rationale at first seems to be logical, such data, when collected and viewed at regular intervals can frequently show such wide variation that trends over time either do not exist or are not easily determined. The reason for this is that specific contaminant sources are often sporadic (e.g. combined sewer outfalls or ocean disposal programs) and the findings of any one survey will be greatly influenced by the nature of both the recent discharge events and physical environment conditions. This would be particularly true for the Seattle area where there are large numbers of contaminant sources all discharging at differing times and rates.

Because of the inherent variability of contaminant data taken close to sources, no attempt was made to correlate contaminant levels along transport pathways immediately next to the shoreline. Furthermore, an analysis that compares levels of contaminants at different localities should, to provide the most valid comparisons, be normalized both for grain-size and for sedimentation rate, two parameters that were not available for this study (see Robertson and O'Connor, 1989, for a full discussion of normalizing procedures). Triangular diagrams of the sediment compositions in the Duwamish River (shown in EPA, 1988c, but used as the data base in Roy F. Weston, Inc., in press) reveal the importance of normalizing for grain-size. The samples collected for their contaminant levels showed a large range of sand and mud contents, and probably for this reason, no meaningful correlations were made between contaminant levels and the sediment transport pathways in the river.

Because of the above difficulties, only two lines of samples that approximate the derived transport paths were chosen for examination. These follow the central axes of the East and West Waterways (Fig 19). Line A, which corresponds to Line 24 (Fig 4), lies on a transport path defined by total deposition. According to the above concepts there should be preferred sites for the deposition of contaminated particles. Such a site is clearly seen at EW-05, a point about two thirds of the way into the East Waterway (Fig. 20). Line B in the West Waterway, on the other hand, lies on a transport path defined by net accretion, an environment which tends to concentrate contaminants in the direction of transport. Thus, contaminant levels should increase from WW-20 in the north to WW-06 in the south, which is, in fact, observed for most of the measured contaminants (Fig. 21).

In the remaining areas of study, contaminants can be expected to behave according to the transport paths for mud (Fig 5). Net accretion dominates in the Elliott Bay clockwise gyre in water depths above 300 feet. Over time, contaminants from all sources will tend to accumulate along these pathways. Despite the very high levels of contaminants found inside the finger docks, there is seldom total deposition occurring. Thus, despite net accretion, the sediments (and contaminants) are mobile and may continue to be transported in the clockwise regime. In the event that contaminant sources could be decreased or eliminated, some "self-cleaning" and eventual burial of contaminants in the sediments could be expected. It must be remembered, however, that sediment supply is very small, and the processes responsible for their movement require extreme events. Even if contaminant sources were eliminated, a "considerable length of time" must surely be required for self-cleaning or burial to become effective.

In depths greater than 300 feet, contaminants that remain associated with the very fine material still present will have equal probability of being deposited anywhere. For this reason, it can be expected that there will be a

low variability in contaminant levels and specific "hot spots" would not be present. This finding is supported by various authors who have studied the distributions of contaminants elsewhere in Puget Sound (e.g. Bloom and Crecelius, 1987)

5.3.3 Sites for Environmental Monitoring

Over time, many contaminants will associate with natural sediment particles and be transported away from the immediate sources either to accumulate or to disperse. Environmental monitoring sites chosen on the basis of long-term contaminant behavior will, therefore, provide data that are less influenced by short term events, and may supply trends that better reflect the health of the environment as a whole.

From the derived transport paths (Fig.5), several locations have been selected as possible monitoring sites (Fig.22). The first site (Site I, Fig.22) is located inside the northeast canyon at the end of the transport gyre. A core at this location should provide the best understanding of "contamination history" in Elliott Bay, as well as provide an important determination of sediment deposition rate. An analysis of surface sediments collected at regular time intervals should reflect the efficacy of contaminant control.

Site II has been selected to parallel the waterfront. It is placed in the principal transport pathway that dominates Elliott Bay and is located at some distance from the docks to avoid the large variabilities that may be induced by local contaminant sources. Because in this area, transport more or less parallels the bathymetric contours, it is suggested that a linear sequence of samples (every 500 m to 1 km) be taken at a depth of 150 feet. Samples, taken at regular time intervals, would provide a clearer understanding of the contaminant behavior with the transport regime, as well as the required trends over time to assess source control programs.

Sites III and IV follow the transport pathways down the central axes of East and West Waterways and are obvious contaminant "traps". The East Waterway (Site III) is in an environment of total deposition and one contaminant high has already been identified (Fig.20). Again, regular sampling would provide the basis to evaluate the effects of source controls.

Site V has been selected simply because it is located at the confluence of two transport regimes and may be receiving contaminants from both the Elliott Bay Waterfront and the Duwamish River. It should, therefore, be a key site to obtain information concerned with both areas

Finally, Site VI at the Turning Basin is believed to be important for the reason that muds are apparently reaching this area from down-river. Not only should this be of concern because of the contaminants that they may be carrying, but there is the added possibility that mud deposition may be increasing as a result of dredging activities.

6.0 SUMMARY AND CONCLUSION

(1) A sediment trend analysis was performed on over 500 grain-size distributions taken from Elliott Bay and the Duwamish River waterway. Mud and sandy muds make up the dominant sediment type and provided the basis for determining the net sediment transport pathways over most of the region. A separate analysis was performed on sands and muddy sands. The two analyses produced essentially identical patterns of transport. When sample sequences contained duplicate samples, the trends were run twice, but no change in interpretation was found to be necessary.

(2) Transport in Elliott Bay is characterized by a clockwise gyre that follows the Seattle Waterfront in less than 300 feet of water. Inside the inner portion of Elliott Bay, the gyre circulates around the PSDDA disposal site and terminates in the deep water of the northeast canyon. In outer Elliott Bay transport bifurcates from the gyre and "fans" westwards into Puget Sound. Sediments in both East and West Waterways appear to be derived from the Elliott Bay transport regime rather than from the Duwamish River. In the river itself, upstream transport of mud could be detected as far as the Turning Basin; however, these trends were weak and not easily interpreted. One stretch of river (Georgetown Reach) showed a reverse direction.

(3) In general, the muddy sediments showed X-distributions indicative of slight net accretion in water depths of less than 300 feet. In most cases, net accretion (rather than total deposition) was also established for sediments inside individual finger docks. Propellor wash is considered to be responsible for resuspending trapped sediments and returning at least a portion back into the main clockwise gyre. Total deposition is evident in East Waterway. In deeper water (300 feet), X-distributions become increasingly horizontal which suggest that the sediments are too fine for further size-sorting (i.e. all particles have an equal probability of deposition). Most of the sand transport trends showed the sediments to be in dynamic equilibrium.

(4) The patterns of sediment transport indicate that shoreline sources are dominant over the Duwamish River source. The latter supplies sediment in a surface plume that circulates in a counterclockwise direction past the Seattle Waterfront. After settling through the pycnocline, Duwamish River sediments are mixed with those derived from shoreline sources after which transport and deposition occur in the reverse direction.

(5) Bottom current measurements show velocities that are generally too low to instigate sediment transport, and their directions show no relationship with the clockwise gyre. Thus, transport must be related to extreme events, probably storms from the south, that are capable of initiating nearshore erosion and transport. Such events would favour the development of a clockwise circulation pattern. Despite the absence of supporting process measurements, bedforms near the Four Mile Rock disposal site verify the existence of sediment movement into Elliott Bay. Furthermore, bedforms have been observed associated with the PSDDA disposal site, again confirming that sediment movement is possible in over 200 feet of water.

(6) It is suggested that the amount of sediment available for transport and deposition, is very small. The supply of sediments from the Duwamish River has steadily decreased during urbanization and is known to be small compared to shoreline sources. The latter, too, are becoming increasingly rare as protective works are used to inhibit erosion. Given that extreme events are necessary for transport to occur, rates of both transport and deposition must be slow over the long-term. For this reason, there has been little observed alteration of most of the anthropogenic disturbances (i.e. the PSDDA disposal site, Harbor Island shipyard deposits etc.)

(7) The trends demonstrate that sediment transport out of disposal sites is possible in water depths above 300 feet, although such dispersal is evidently very slow. Below 300 feet, further transport of disposed material is extremely unlikely. Such sites would eventually become buried by fine material coming out of suspension.

(8) The presence of mud in the Turning Basin that appears to have come from downriver should be a source of concern. If correct, these deposits are transported by "tidal pumping", a process that is augmented by dredging. The samples taken for this study suggest that sand in the Duwamish River is becoming increasingly rare, and its removal may result in favoring the deposition of mud that, having come from Elliott Bay and the lower Duwamish River, will undoubtedly contain contaminants. (9) Only two lines of contaminant data were used to correlate with the derived transport paths. The findings were essentially as predicted, lending support to the validity of the trends. In East Waterway, an environment of total deposition, a contaminant high was observed in its southern half (i.e. there is a preferred location where contaminated particles are deposited, after which there is no further transport). In West Waterway, an environment of net accretion, contaminants generally increased from north to south demonstrating that transport processes, rather than a specific source, are responsible for concentrating contaminants.

(10) The derived transport pathways are used to locate six regions where future environmental monitoring may be most effective. These have been chosen at the ends of transport paths and along specific transport pathways that best characterize the environment. It is felt that monitoring should be undertaken away from specific sources to minimize local variability and to produce a data base capable of deriving long-term trends.

7.0 ACKNOWLEDGMENTS

Sincere appreciation is extended to Dr. Teresa Michelsen of the Washington Department of Ecology who first became interested in the approach of sediment trends and was instrumental in establishing this project. She also organized funding and acted as scientific authority.

Special thanks are extended to Laura Lowe (Ecology), Mike Francisco (NOAA), John Malek (EPA), Gene Revelas (Department of Natural Resources), Doug Hotchkiss (Port of Seattle), David Kendall (US Corps), Nancy Musgrove and Steve Fuller (Weston), and other members of the Elliott Bay/Duwamish Restoration Panel for fund support and helpful discussions during the course of the project.

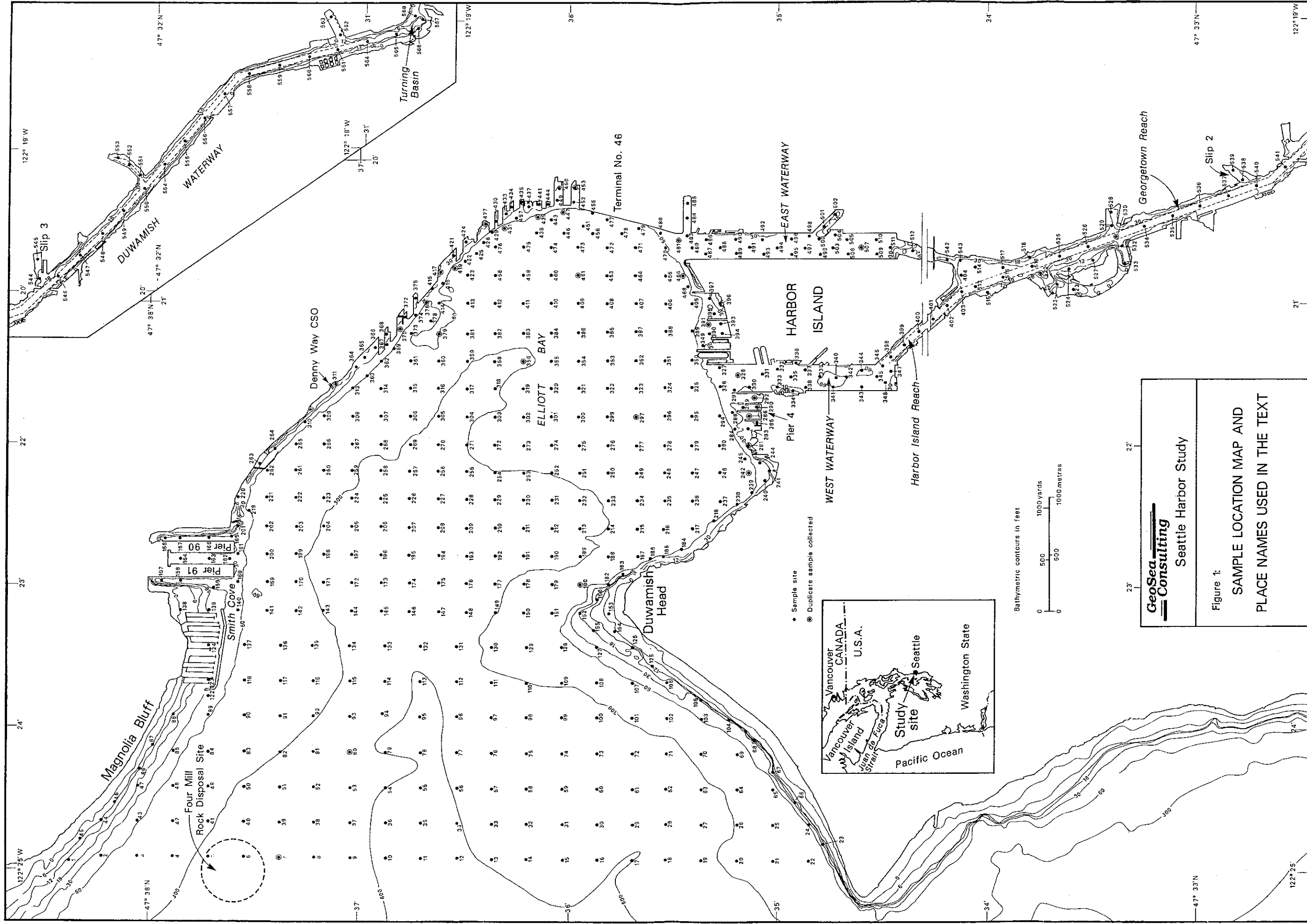
The help of Lou Schwartz, skipper of the BRENDON "D" II (Sound Vessels Inc.) in collecting the samples is gratefully acknowledged. All grain size analyses were carried out by Richard Powys (GeoSea).

8.0 REFERENCES

- Baker, E.T., 1982: Suspended particulate matter in Elliott Bay; NOAA Technical Report ERL 417-PMEL 35, 44 p.
- Baker, E.T., Cannon, G.A. and Curi, H.C., 1983: Particle transport processes in a small marine bay; *Journal of Geophysical Research*, Vol 88, 9661-9669.
- Black, K.P. and Barnett, A.G., 1988: Sediment transport modeling under tidal flows with applications in a natural estuary; LAHR Symposium on Mathematical Modeling of Sediment Transport in the Coastal Zone. Proceedings. Copenhagen, May 30 - June 1, 1988, 5-13.
- Blomberg, G., Simenstad, C. and Hickey, P., 1988: Changes in the Duwamish River Estuary habitat over the past 125 years; *Proceedings, First Annual Meeting on Puget Sound Research, Vol. 2*: Published by the Puget Sound Water Quality Authority, 217 Pine St., Suite 1100, Seattle, Wash., 98101, 437-454.
- Bloom, N.S., and Crecelius, E.A., 1987: Distribution of silver, mercury, lead, copper and cadmium in central Puget Sound sediments; *Marine Chemistry*, Vol 21, 377-390.
- Cooper Consultants, Inc., 1986: Checking studies on zones of siting feasibility for dredged material disposal in Puget Sound; Unpublished report to U.S. Environmental Agency, Region 10.
- Cox, J.M., et al., 1981: Index to observations of currents in Puget Sound, Washington, from 1908-1980; NOAA Technical Memo, OMPA-5, 51p.
- Curl, H.C., 1982: Estuarine and coastal pollutant transport and transformation, the role of particulates; FY 80-82 Final Report, Pacific Marine Environmental Laboratory, Seattle Wash. 98115, 228p.
- Curl, H.C. et al., 1988: Contaminant transport from Elliott and Commencement Bays. NOAA Technical Memorandum ERL PMEL-78, 136 p.
- De Meyer, Ph. and Wartel, S., 1988: Relation between superficial sediment grainsize and morphological features of the coastal ridges off the Belgium coast; in: De Boer, P.L., et al. (eds), *Tide Influenced Sedimentary Environments and Facies*, Dordrecht, Riedel, 91-100.
- Downing, J., 1983: *The Coast of Puget Sound, its Processes and Development*; Puget Sound Books, 126 p.
- Environmental Protection Agency, 1988a: Characterization of spatial and temporal trends in water quality in Puget Sound; Puget Sound Estuary Program, EPA 503/3-88-003, Region 10, Office of Puget Sound, Seattle, WA, 98101.

- Environmental Protection Agency, 1988b: Evaluation of potential contaminant sources; Elliott Bay Action Program, prepared by Tetra Tech, Inc.
- Environmental Protection Agency, 1988c: Analysis of toxic problem areas; Elliott Bay Action Program, prepared by PTI Environmental Services and Tetra Tech, Inc.
- Environmental Protection Agency, 1993: Harbor Island draft remedial investigation report (Sediment); unpublished report by Roy F. Weston Inc., for EPA Region 10.
- GeoSea Consulting (Canada) Ltd., 1993: Sediment grain size analyses of sediment samples from Elliott Bay, Washington; Report and disk to: Washington Department of Ecology, N.W. Regional Office, 3190-160th Ave., S.E., Bellevue, Wash. 98008. Attn. Dr. T. Michelsen.
- Jenson, J., and Sieffert, W., 1994 (in press): Water level changes in tidal estuaries due to deepening of navigation channels and sea level variations; International Symposium on Water Resources Planning in a Changing World, June 28-30, 1994, Karlsruhe, Germany.
- Little, D.I., and McLaren, P., 1989: Sediment and contaminant transport in Milford Haven, Wales; in: Ecological Impacts of the Oil Industry, B. Dicks ed., John Wiley & Sons, 203-234.
- McGary, N., and Lincoln, J.H., 1977: Tide Prints, Surface Tidal Currents in Puget Sound; University of Washington Press, Seattle and London, 51 p.
- McLaren, P. and Bowles, D., 1985: The effects of sediment transport on grain-size distributions. *Journal of Sedimentary Petrology*, Vol. 55, 457-470.
- McLaren, P. and Little, D., 1987: The effects of sediment transport on contaminant dispersal: an example from Milford Haven. *The Marine Pollution Bulletin*, Vol. 18, 586-594.
- McLaren, P., Collins, M.B., Gao, G., and Powys, R., 1993: Sediment dynamics of the Severn Estuary and inner Bristol Channel; *Journal of the Geological Society*, London, Vol. 150, 589-603.
- McLaren, P., and Powys, R., 1989: The use of sediment trends to assess the fate of dredged material; Proceedings of WODCON XII, World Dredging Congress, Orlando, Florida, USA, 2-5 May, 1989, 223-233.
- McLaren, P., Cretney, W.J., and Powys, R., 1993: Sediment pathways in a British Columbia Fjord and their relationship with particle-associated contaminants; *Journal of Coastal Research*, Vol. 9, 1026-1043.
- Paulson, A.J., Feely, R.A., Curl, C. Jr., and Tennant, D.A., 1989: Estuarine transport of trace metals in a buoyant riverine plume; *Estuarine, Coastal and Shelf Science*, Vol. 28, 231-248.

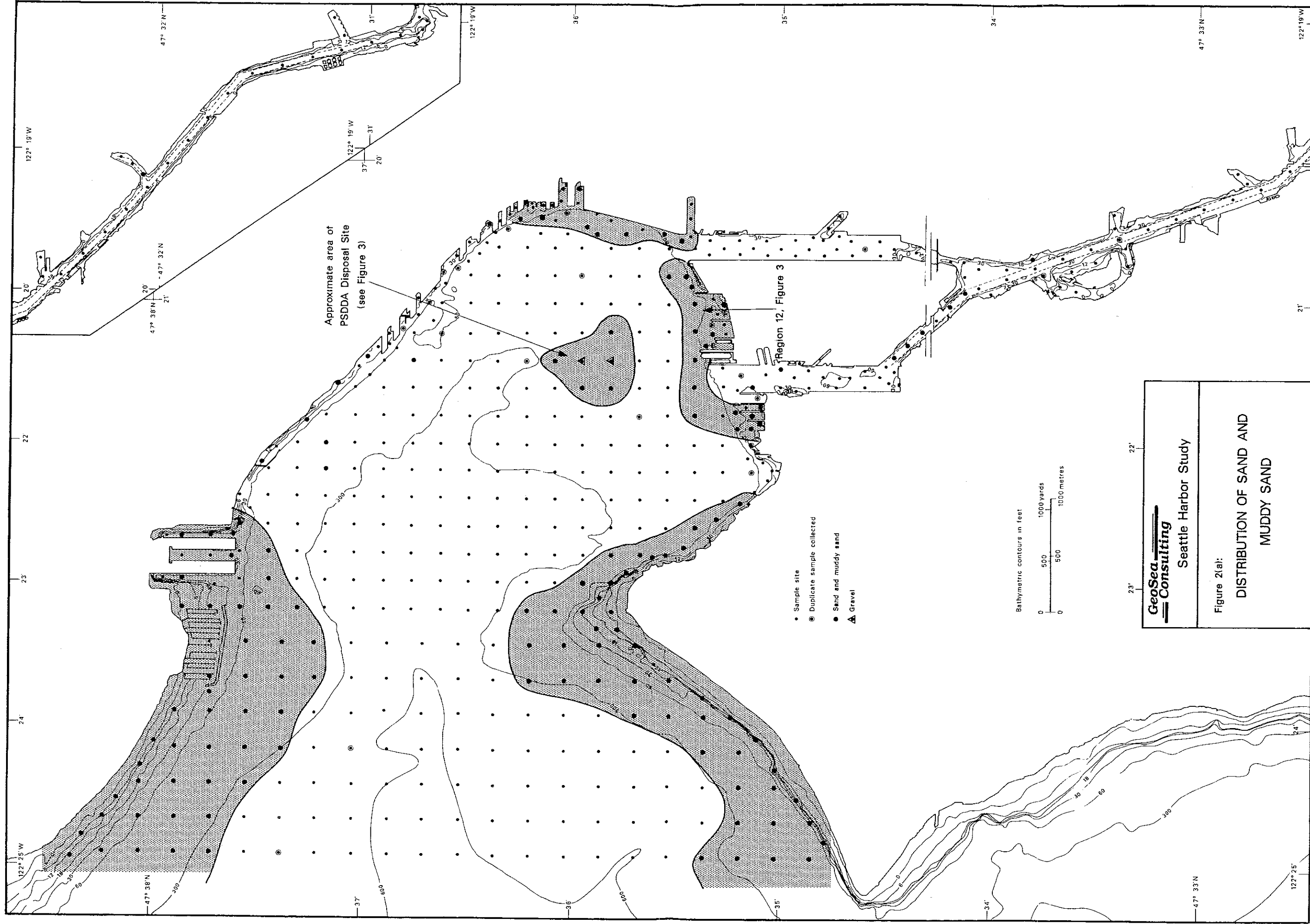
- Revelas, E.C., Kendall, D.R., Nelson, E., Rhoads, D.C., and Germano, J.D., 1991: Post-disposal mapping of dredged material in Port Gardner and Elliott Bay; Puget Sound Research '91 Proceedings; publ. by Puget Sound Water Quality Authority, Mail Stop PV-15, Olympia, WA, 276-280.
- Roberts, R.W., 1979: Subtidal grain size map of Puget Sound. Surface sediments map; Department of Oceanography, University of Washington.
- Robertson, A., and O'Connor, T.P., 1989: National status and trends program for marine environmental quality; aspects dealing with contamination in sediments. In: Contaminated Marine Sediments-Assessment and Remediation. National Academy Press, Washington, D.C., 47-62.
- Rogers, E.H., 1955: A pollution study of Puget Sound using a hydraulic model; M.S., Department of Oceanography, University of Washington, Seattle, 120p.
- Roy F. Weston, Inc., in press: Remedial Investigation Report, Harbor Island, (Part 2 - Sediments); Vols. 1-3. Prepared for U.S. Environmental Protection Agency, Region X, Seattle, Wash.
- Sillcox, R.L., Geyer, W.R., and Cannon, G.A., 1981: Physical transport processes and circulation in Elliott Bay; NOAA Technical Memorandum OMPA-8, Office of Marine Pollution Assessment, Boulder, CO, 45pp.
- Sumeri, A. and Romberg, P., 1991: Contaminated bottom sediment capping demonstration; Puget Sound Research '91 Proceedings; publ. by Puget Sound Water Quality Authority, Mail Stop PV-15, Olympia, WA, 507-520.
- URS Engineers and Evans-Hamilton, 1986: Elliott Bay Oceanographic Studies: Final Report. Prepared for the Municipality of Metropolitan Seattle.
- Van Heuvel, T., McLaren, P., and Powys, R., 1993: Sediment transport pathways in the Eems Estuary, The Netherlands; Proceedings of the 1993 Canadian Coastal Conference, May 4-7, 1993, Vancouver, British Columbia, 167-176.
- Winter, D.R., 1977: Studies of circulation and primary production in deep inlet environments; EPA-600/3-77-049, 100p.



GeoSea Consulting
Seattle Harbor Study

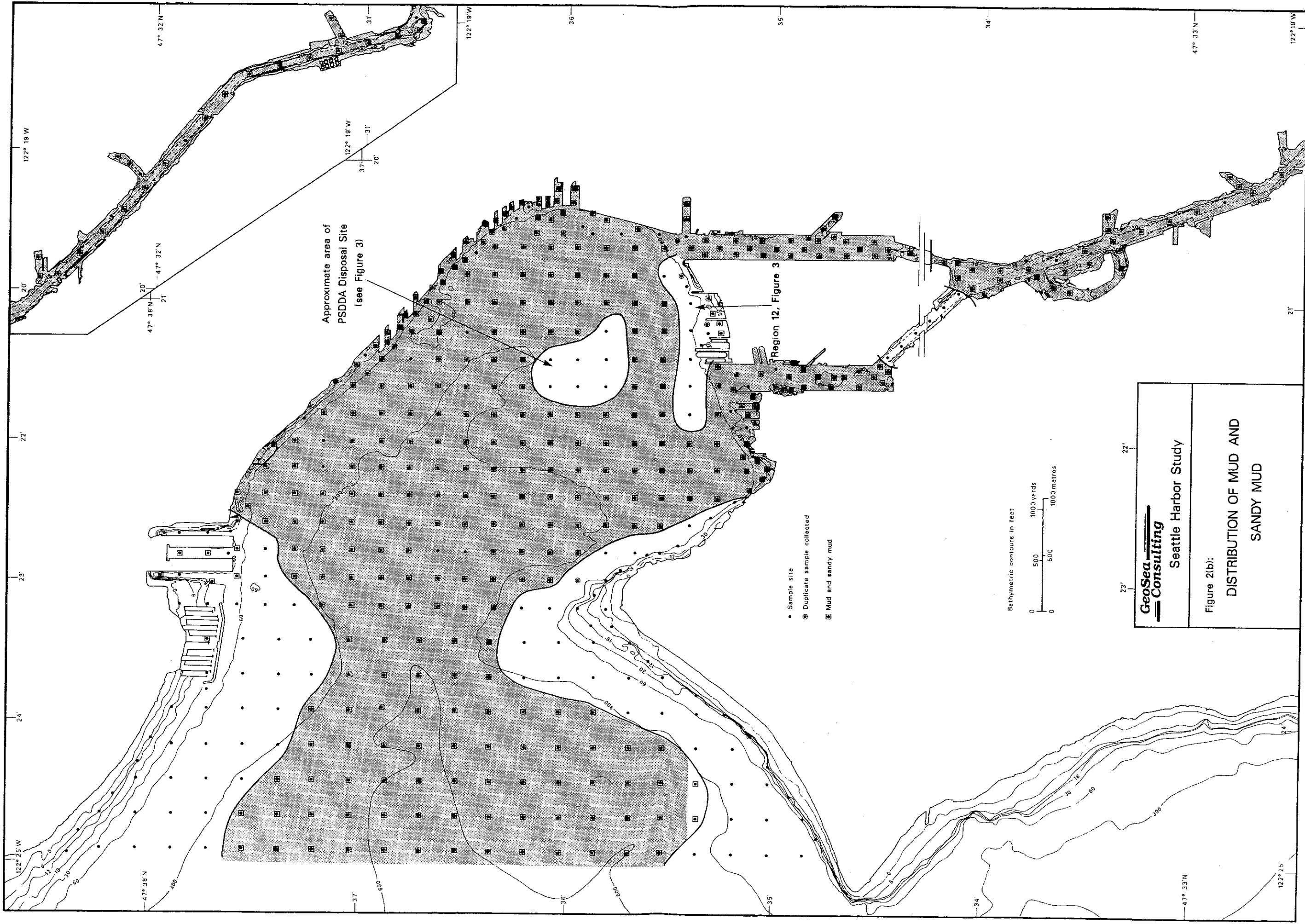
Figure 1:
SAMPLE LOCATION MAP AND
PLACE NAMES USED IN THE TEXT





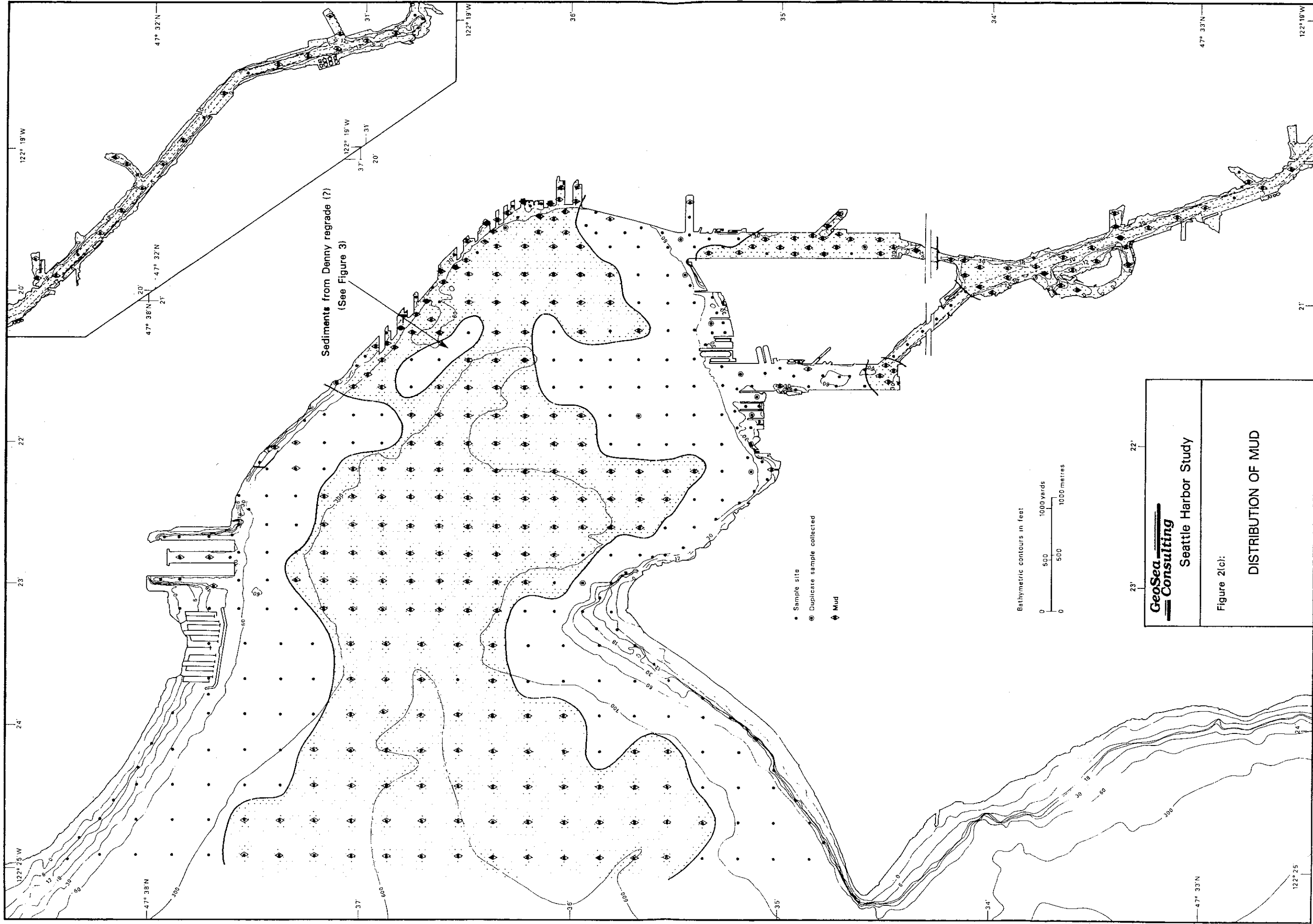
GeoSea Consulting
 Seattle Harbor Study

Figure 2(a):
 DISTRIBUTION OF SAND AND
 MUDDY SAND



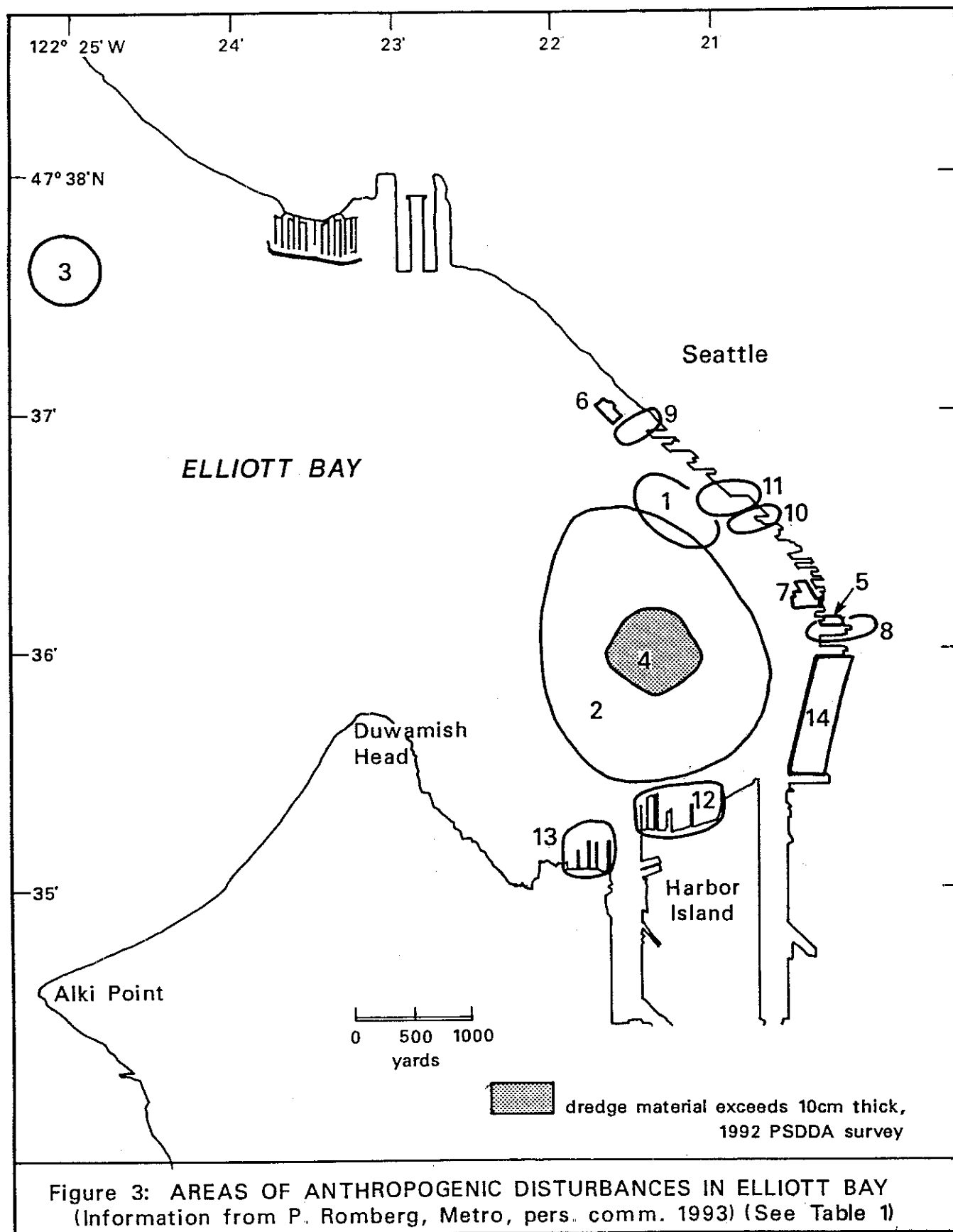
GeoSea Consulting
 Seattle Harbor Study

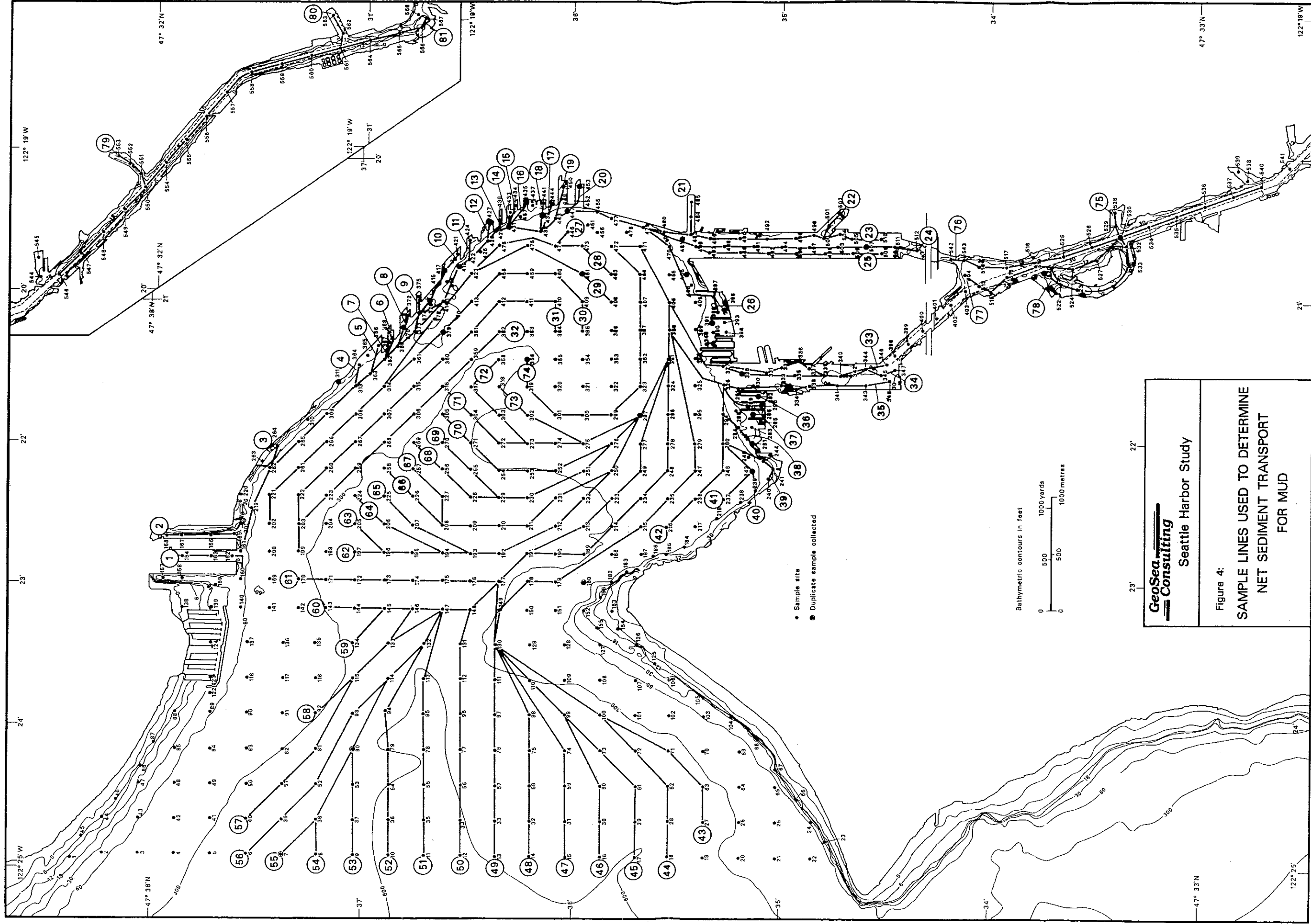
Figure 2(b):
 DISTRIBUTION OF MUD AND SANDY MUD



GeoSea Consulting
 Seattle Harbor Study

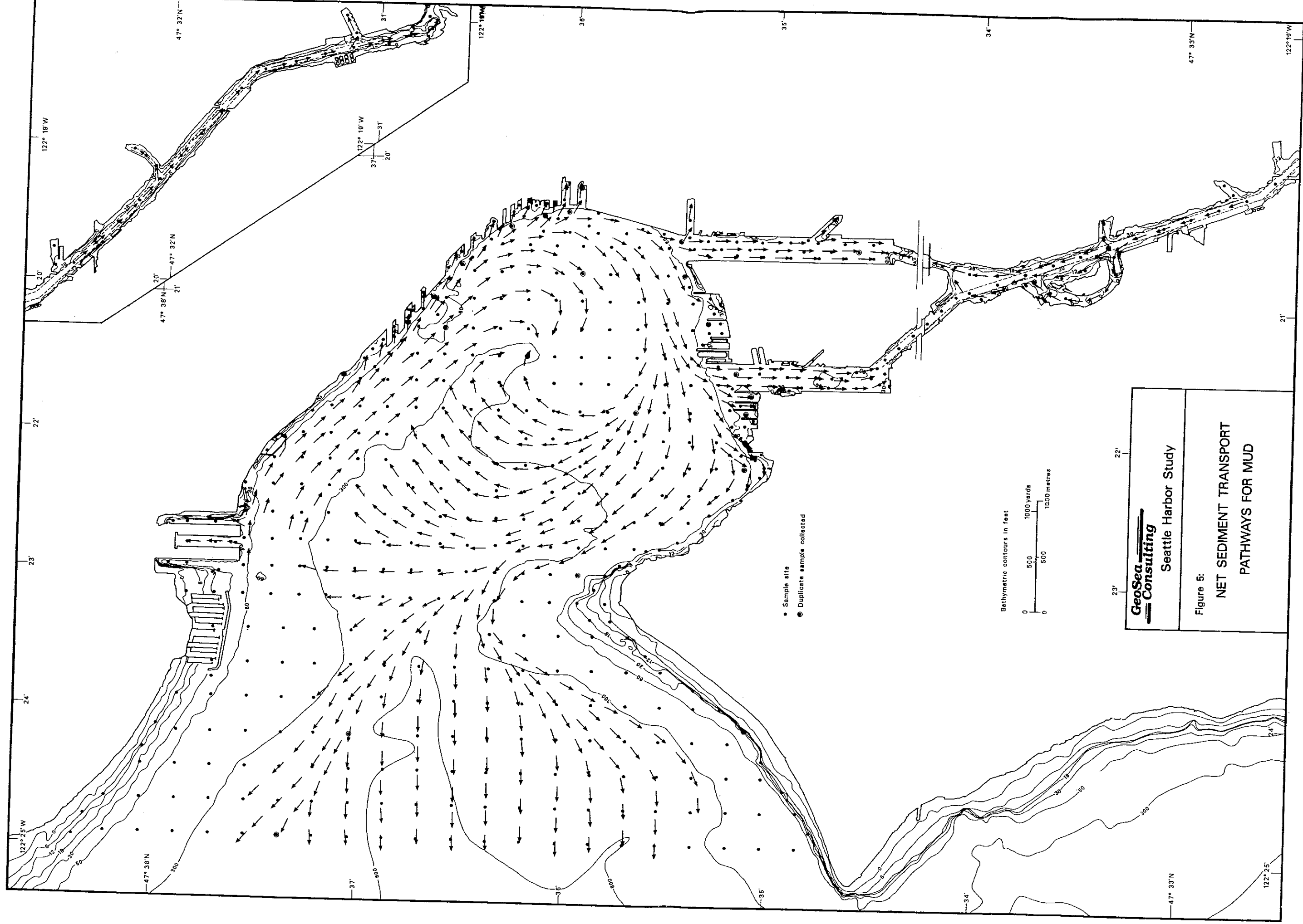
Figure 2(c):
 DISTRIBUTION OF MUD





GeoSea Consulting
 Seattle Harbor Study

Figure 4:
**SAMPLE LINES USED TO DETERMINE
 NET SEDIMENT TRANSPORT
 FOR MUD**



- Sample site
- ⊙ Duplicate sample collected

Bathymetric contours in feet
 0 500 1000 yards
 0 500 1000 metres

GeoSea Consulting Seattle Harbor Study
Figure 5: NET SEDIMENT TRANSPORT PATHWAYS FOR MUD

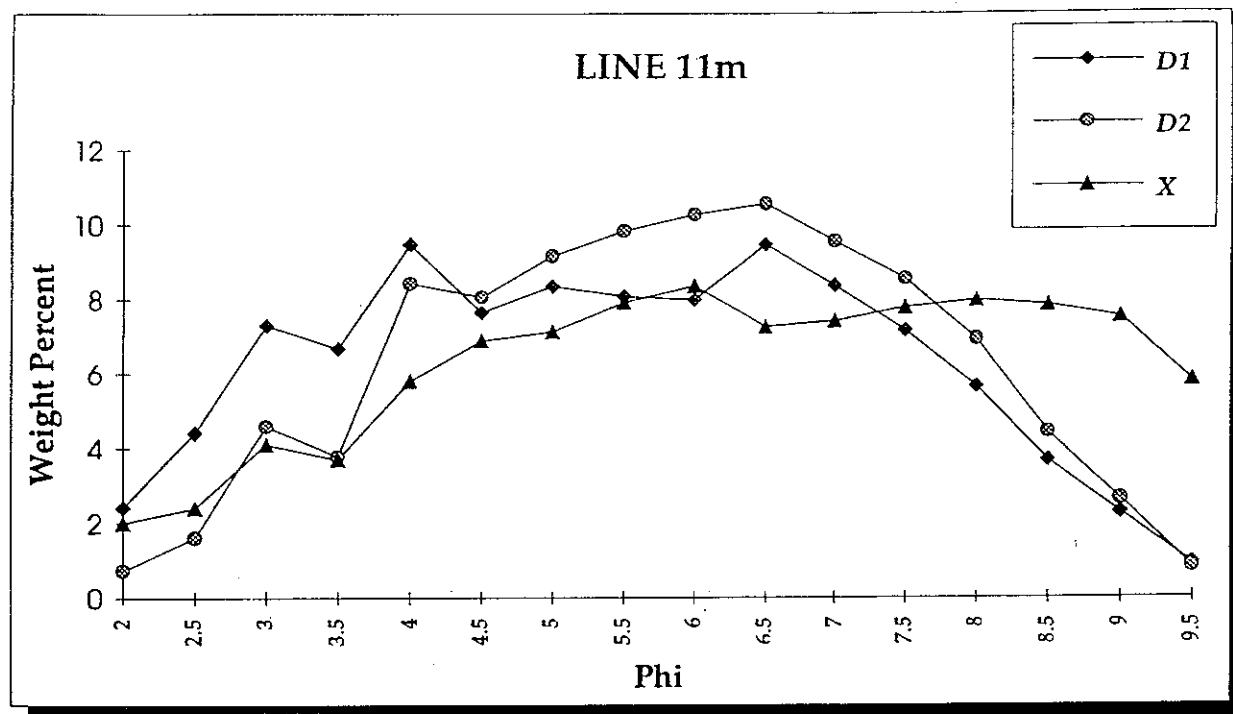


Figure 6: D₁, D₂ and X for Line 11m. The mode of the X-distribution indicates that the sediments are in dynamic equilibrium along the transport path; however, the tail which contains a fine mode suggests slight accretion of the mud component.

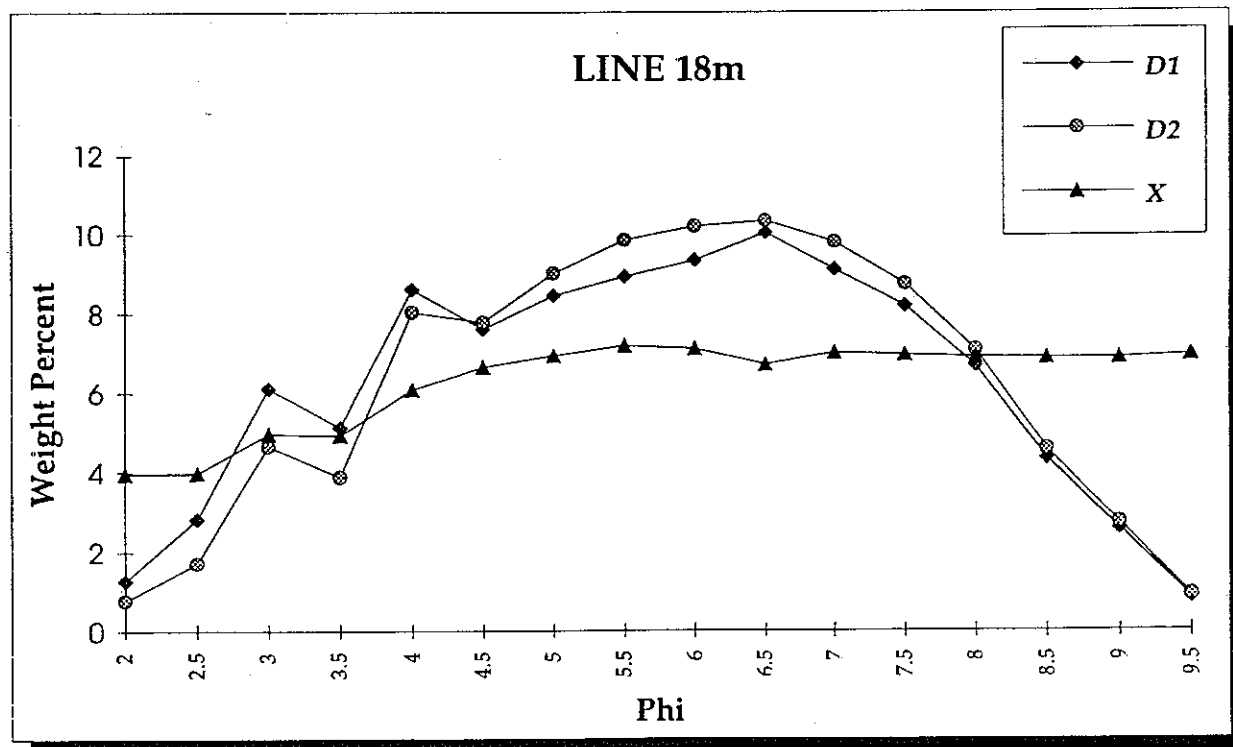


Figure 7: D₁, D₂ and X for Line 18m. The X-distribution is near-horizontal over the mud portion suggesting that fines are no longer being sorted by size.

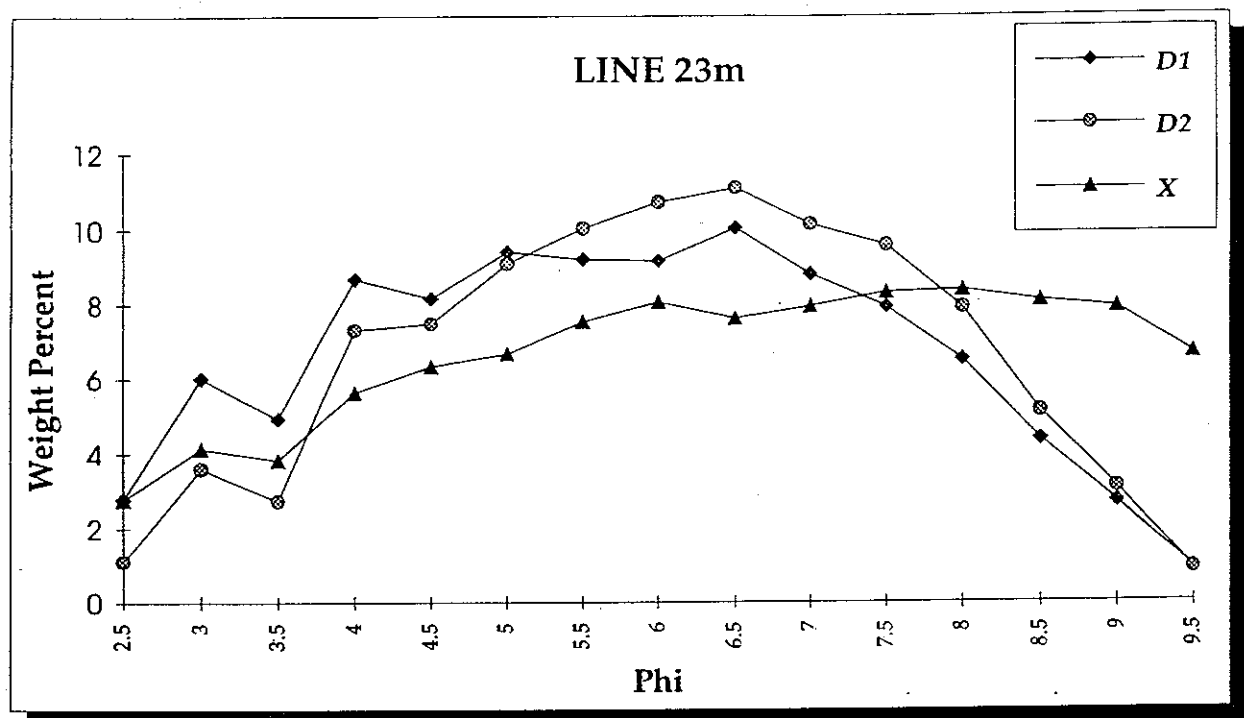


Figure 8: D₁, D₂ and X for Line 23m. The X-distribution increases over most of the D₁ and D₂ distributions suggesting total deposition.

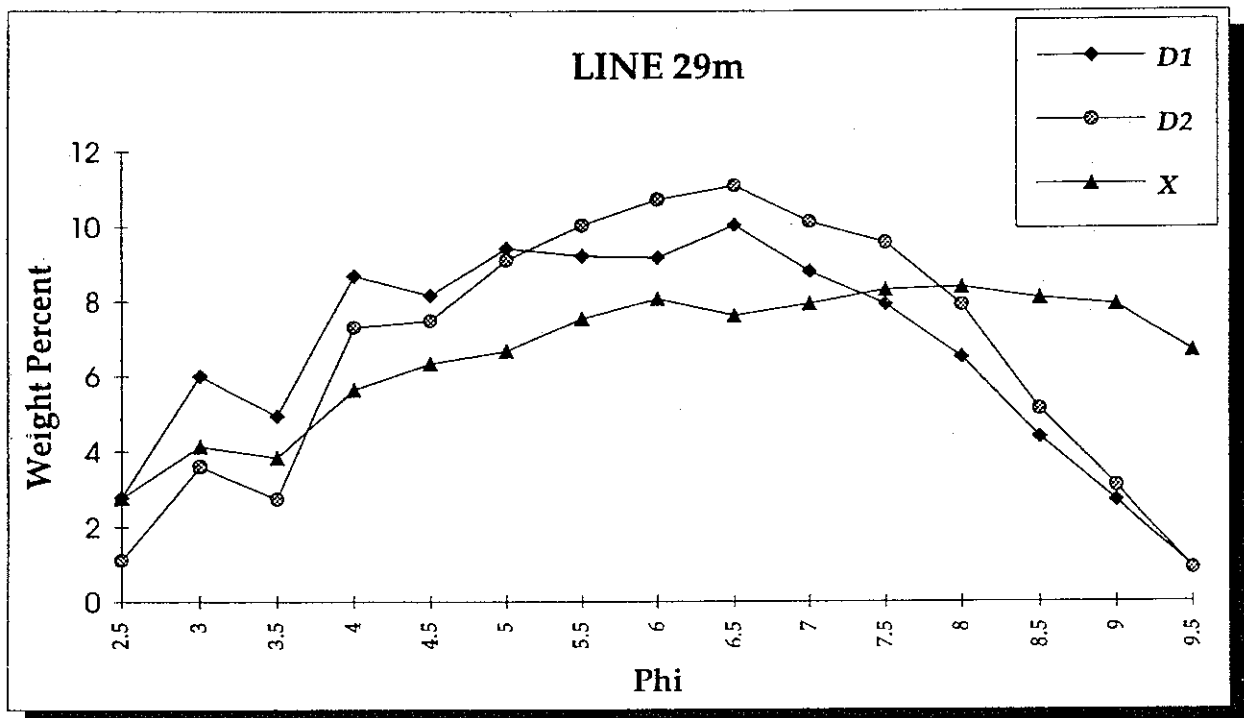


Figure 9: D₁, D₂ and X for Line 29m indicating net accretion along the transport path.

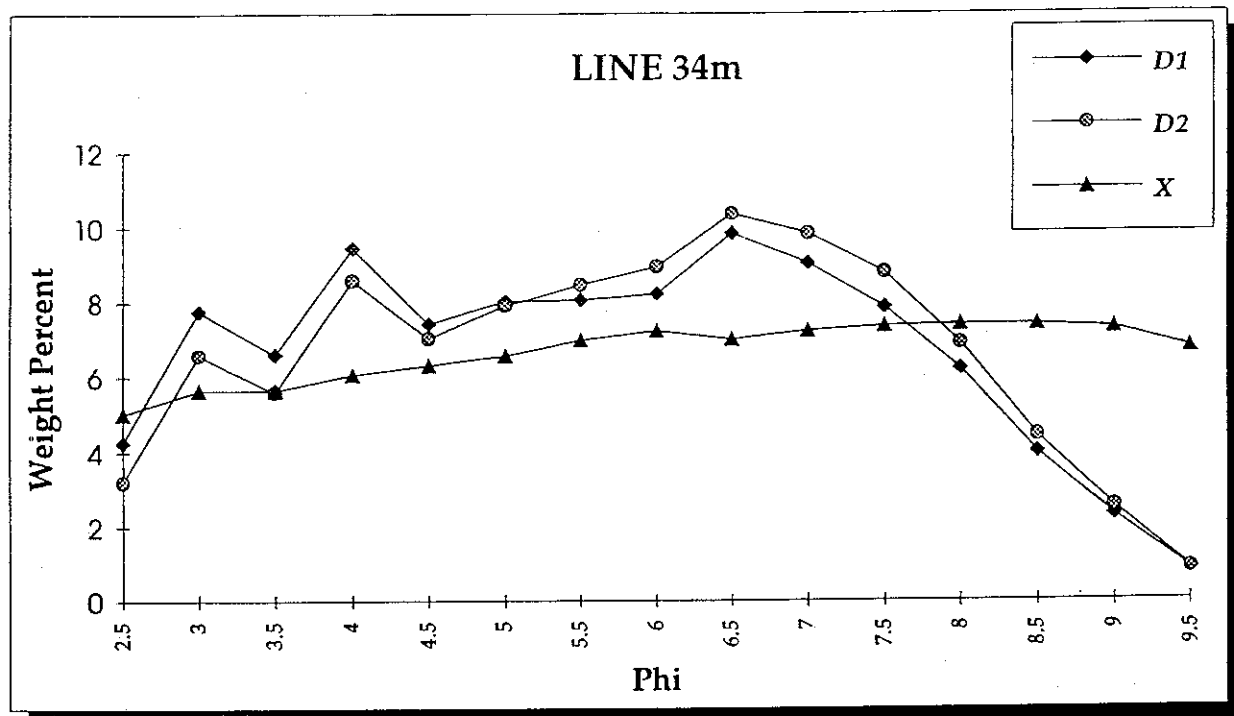


Figure 10: D₁, D₂ and X for Line 34m. Although the mode of X is finer than D₁ and D₂, it is poorly defined and suggests only slight net accretion

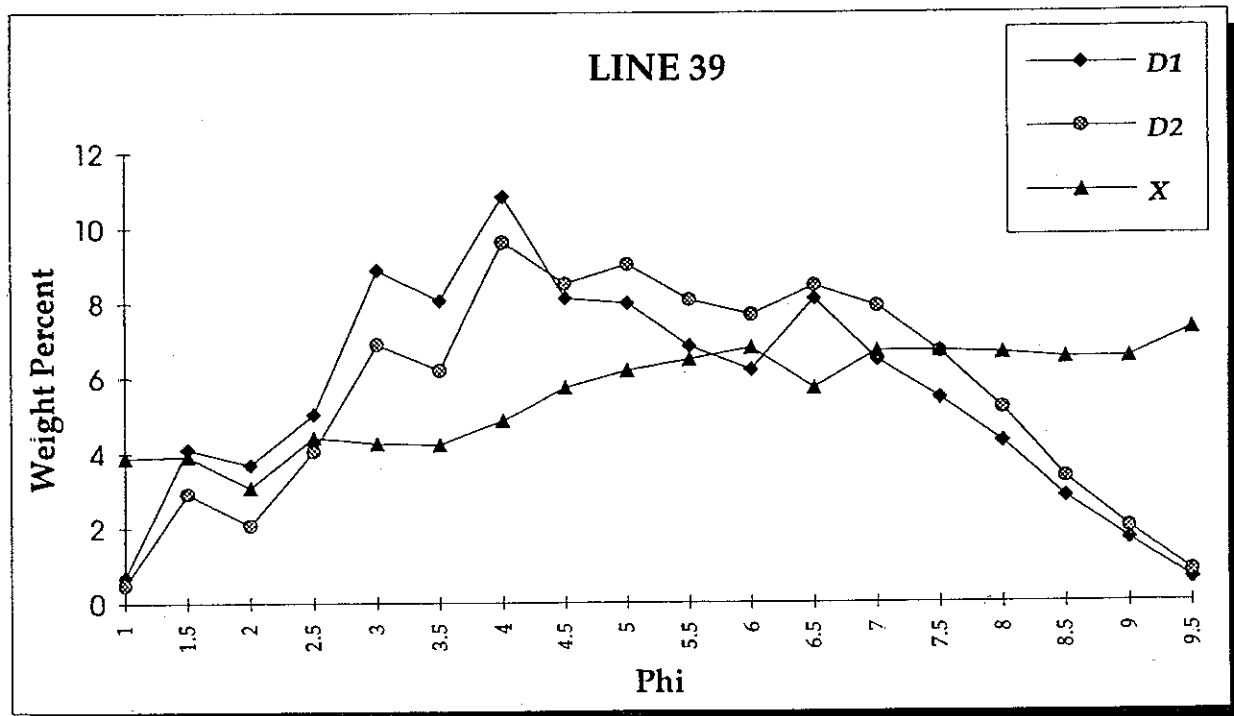


Figure 11: D₁, D₂ and X for Line 39m. The rising X-distribution suggests total deposition.

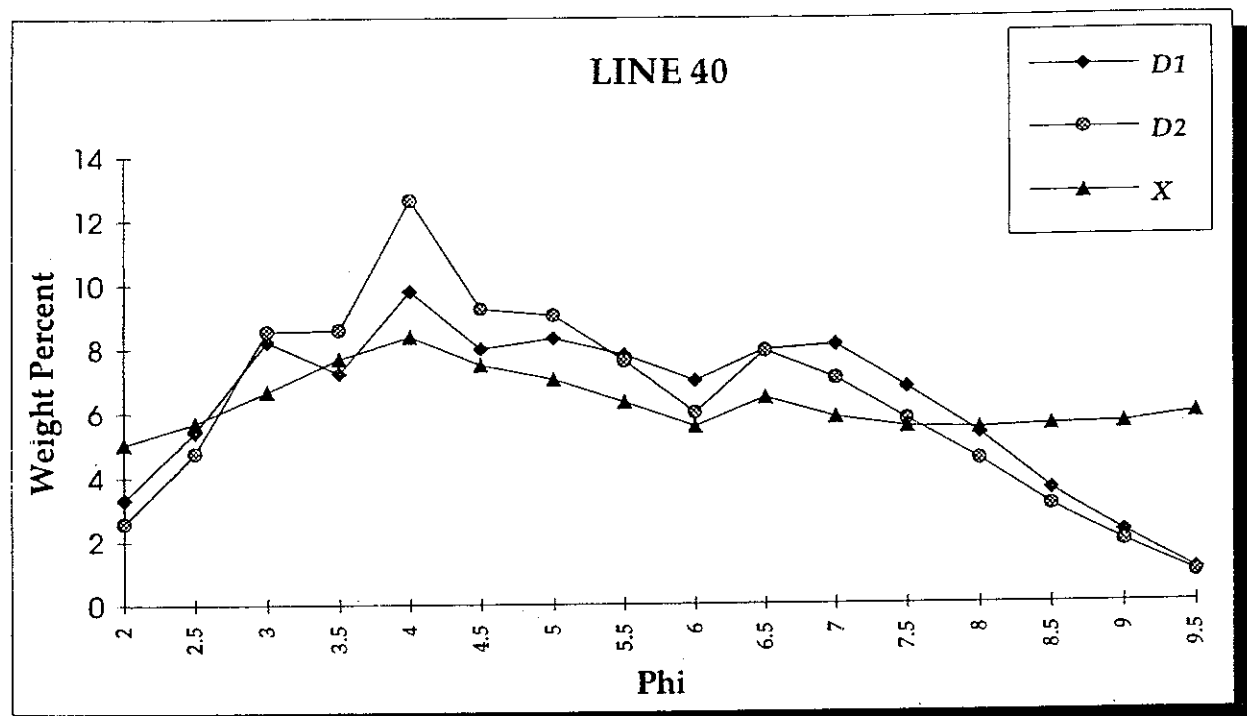


Figure 12: D₁, D₂ and X for Line 40m showing dynamic equilibrium

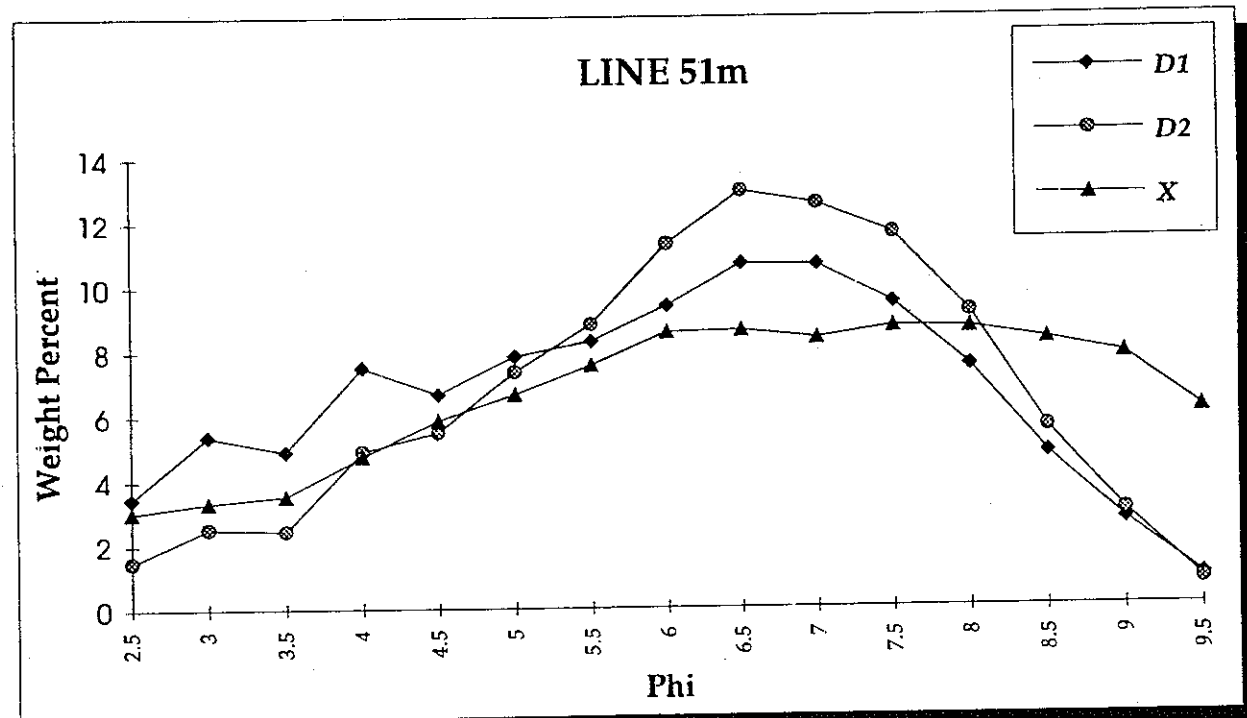


Figure 13: D₁, D₂ and X for Line 51m. The X-distribution suggests slight net accretion.

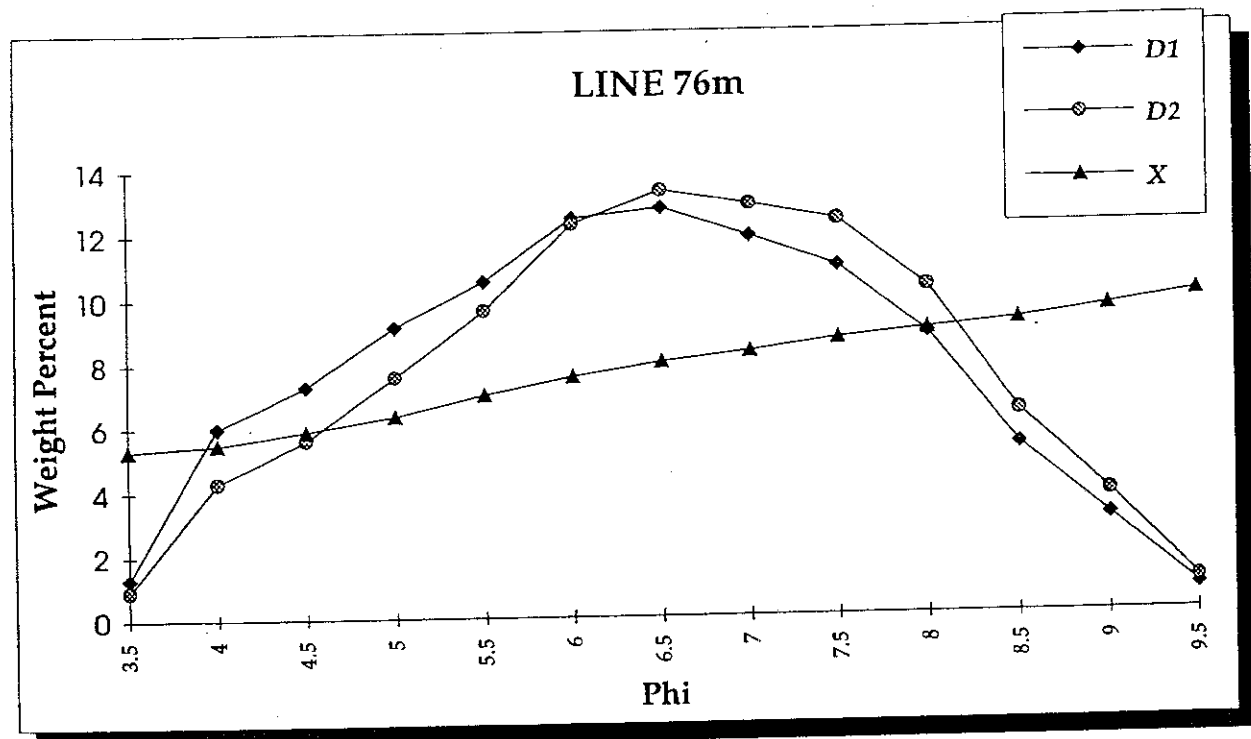
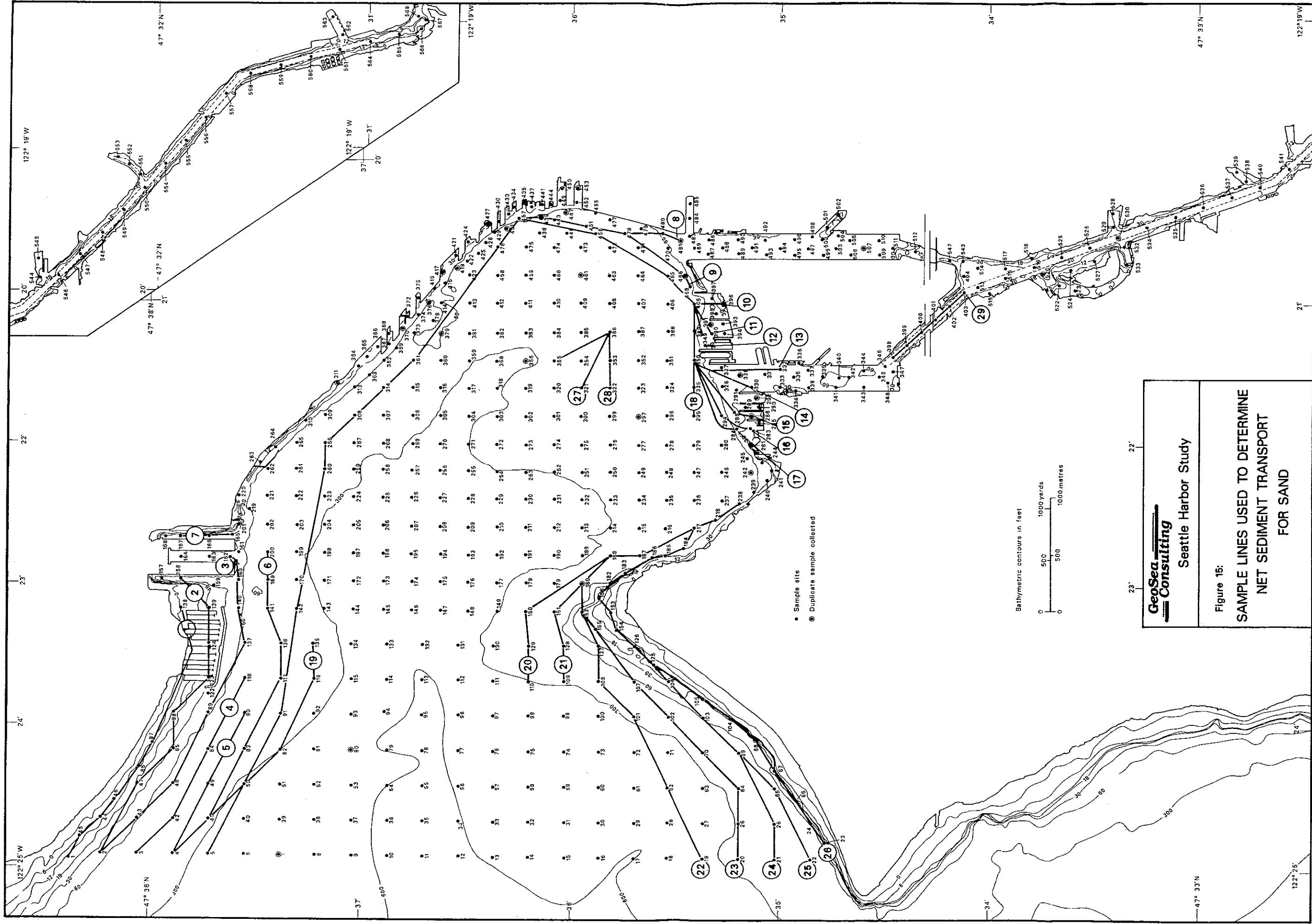


Figure 14: D₁, D₂ and X for Line 76m. The monotonically increasing X-distribution indicates an environment of total deposition.



GeoSea Consulting
 Seattle Harbor Study

Figure 16:
 SAMPLE LINES USED TO DETERMINE
 NET SEDIMENT TRANSPORT
 FOR SAND



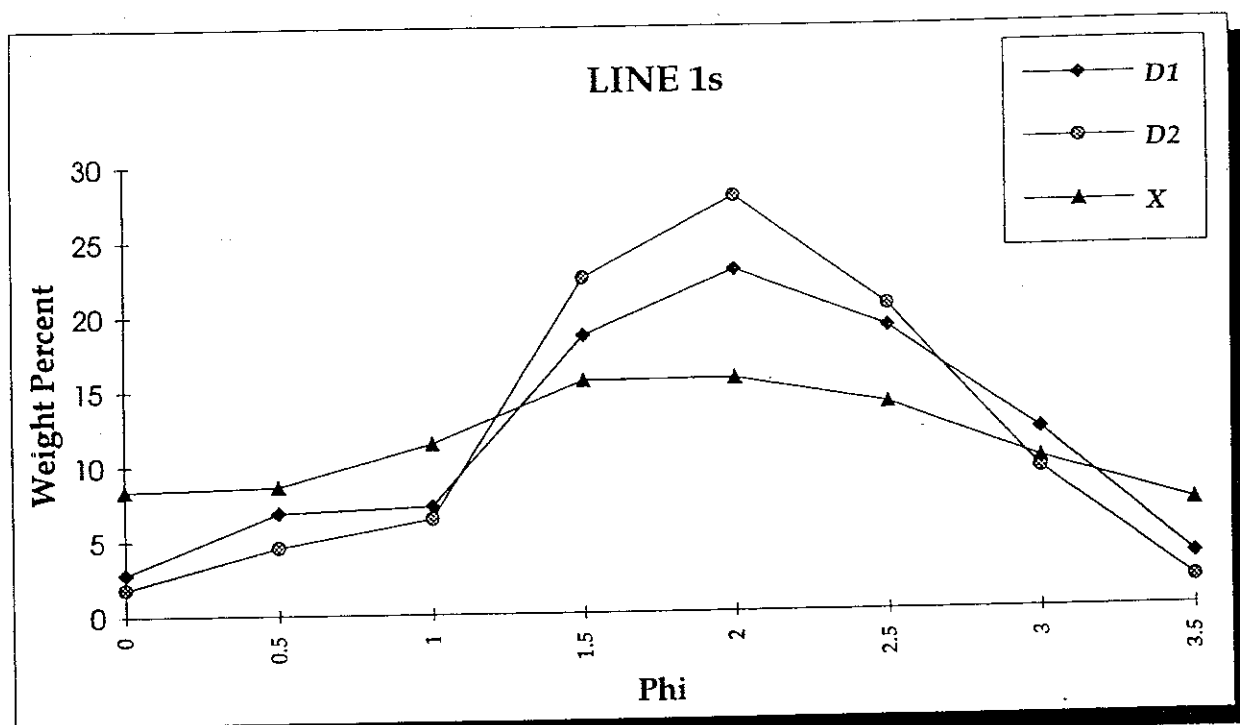


Figure 17: D₁, D₂ and X for Line 1s. The mode of the X-distribution is coarser than the mode of D₁ and D₂ indicating net erosion along the transport path.

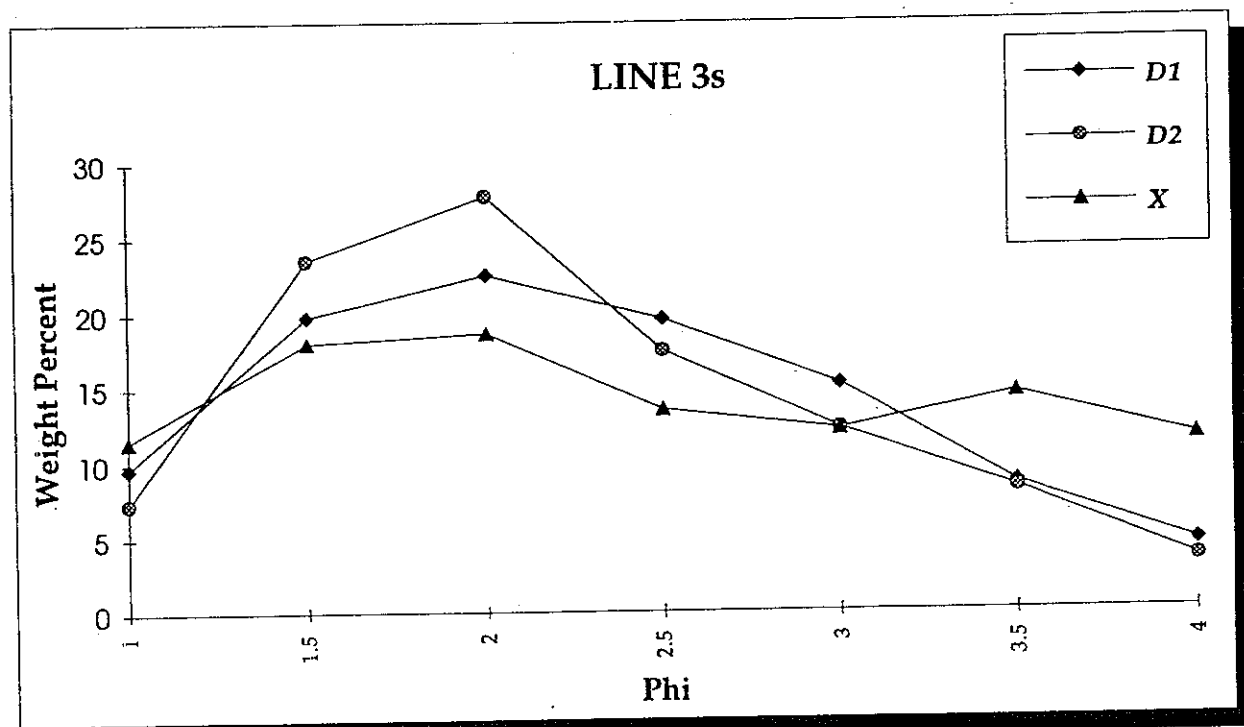


Figure 18: D₁, D₂ and X for Line 3s. The mode of the X-distribution is the same as the modes of D₁ and D₂ indicating dynamic equilibrium.

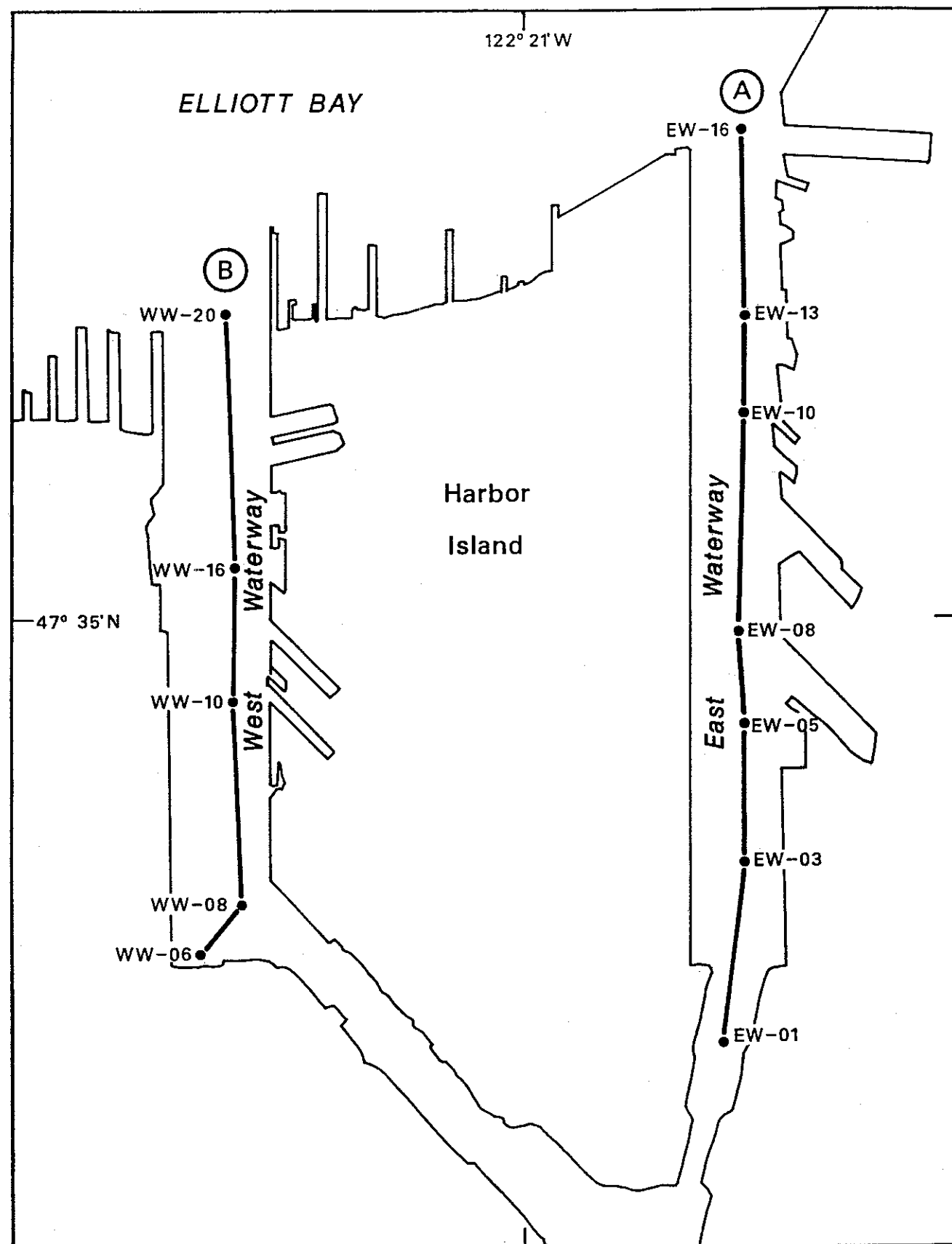


Figure 19: SAMPLE LOCATIONS FOR HEAVY METAL CONCENTRATIONS (EPA, 1993) Lines A and B follow the transport pathways defined by lines 24 and 34 respectively (Fig. 4)

Figure 20
HEAVY METAL CONCENTRATIONS WITH DISTANCE - EAST WATERWAY
 Data from EPA (1993)

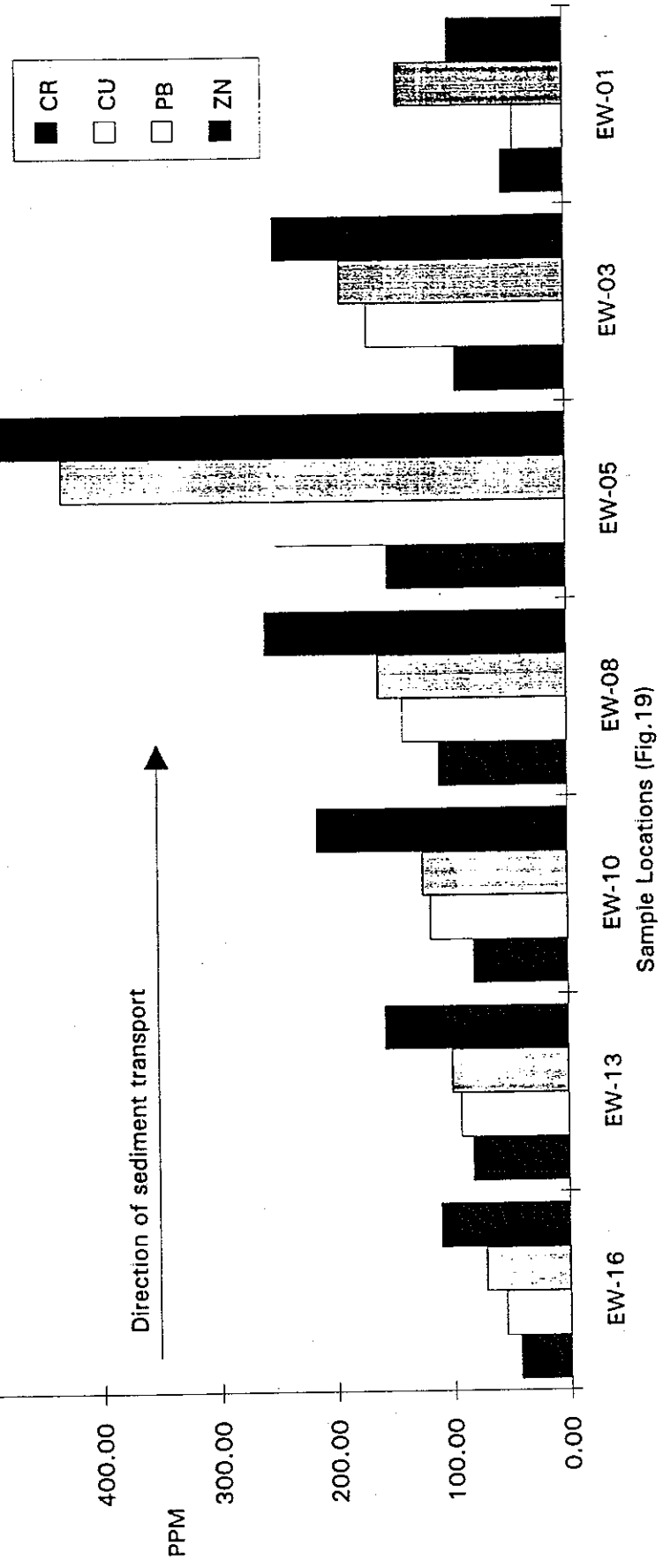
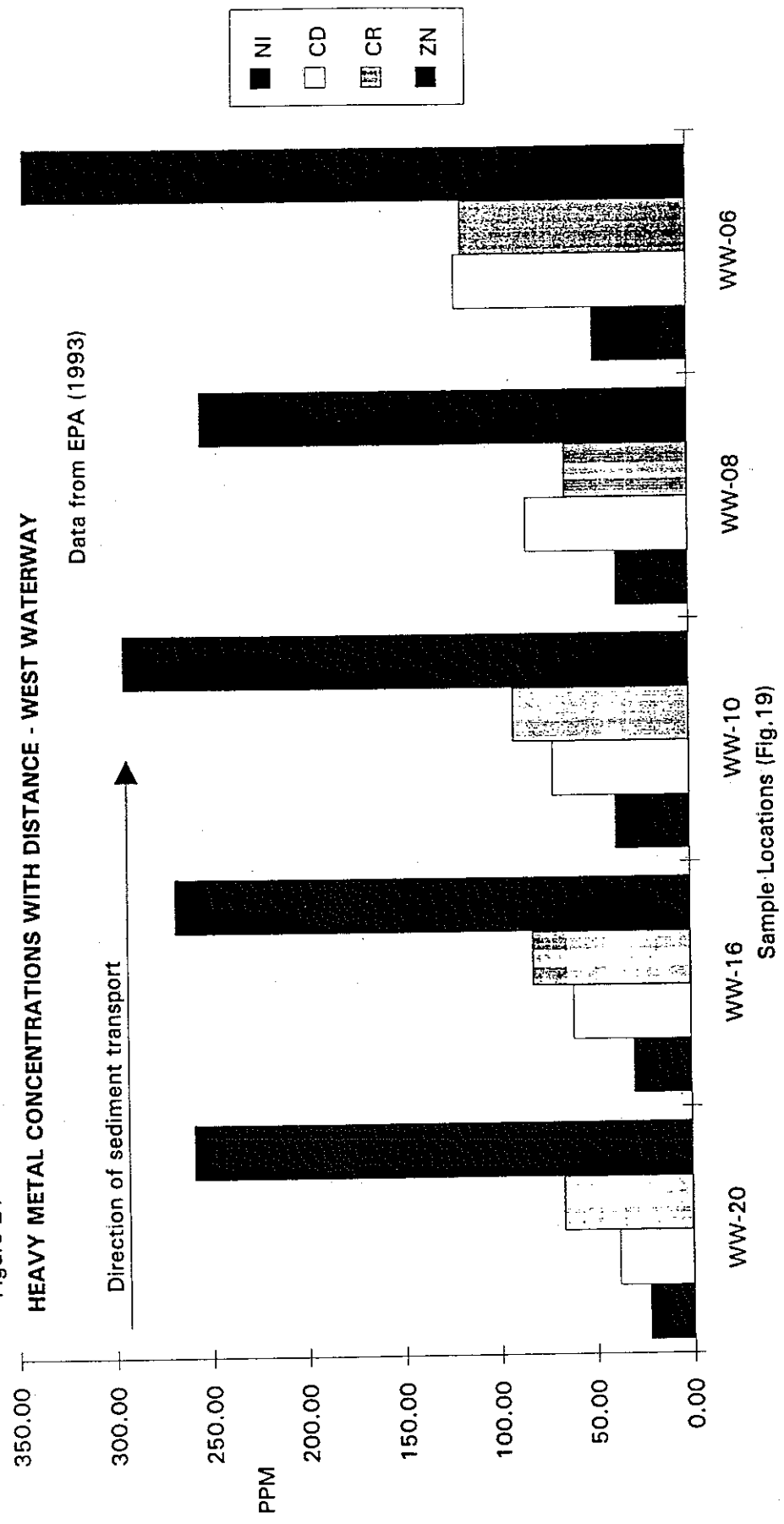


Figure 21

HEAVY METAL CONCENTRATIONS WITH DISTANCE - WEST WATERWAY



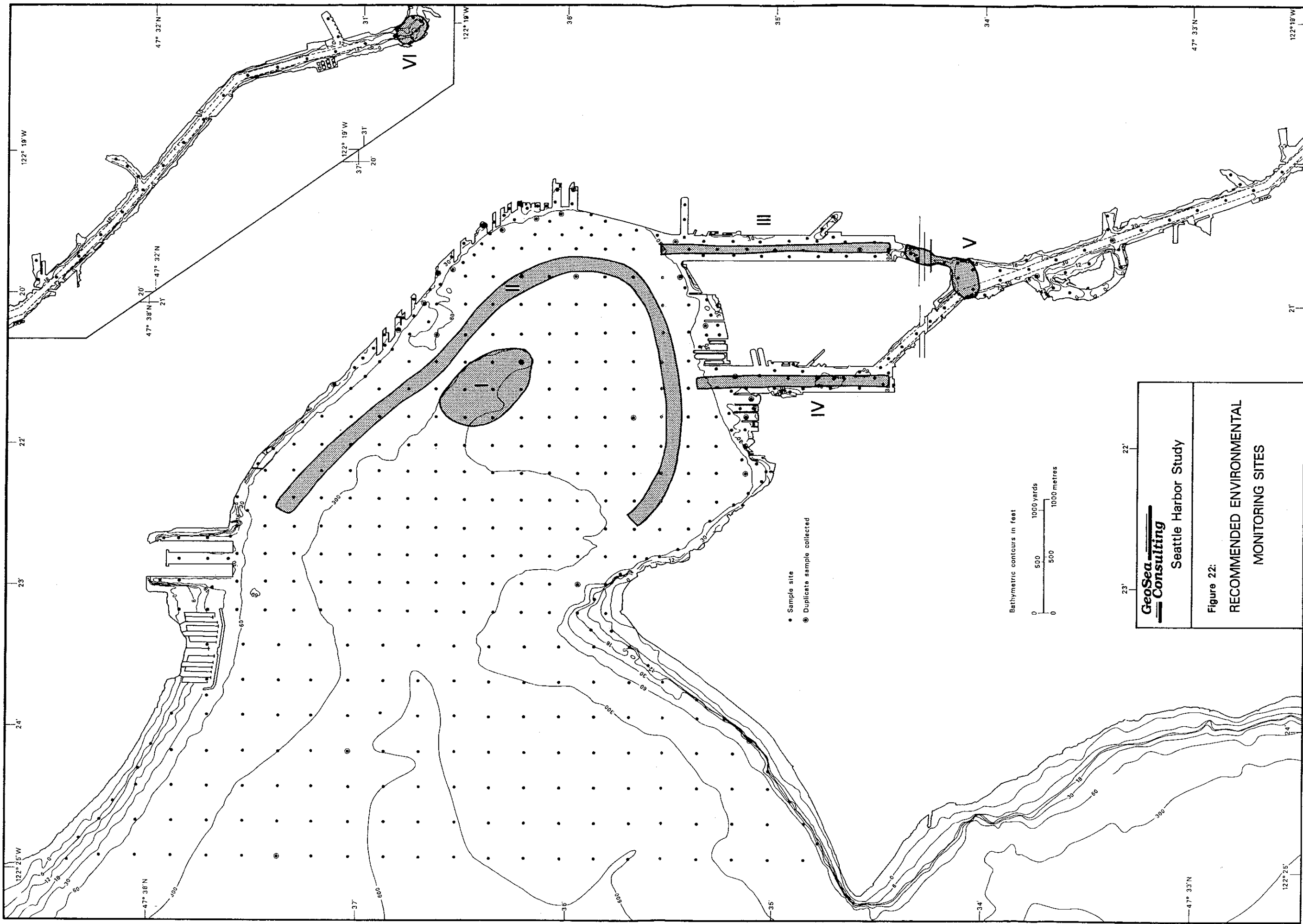


TABLE 1 (1)

PARTIAL LIST OF AREAS OF ANTHROPOGENIC DISTURBANCES (SEE FIGURE 3)

Location	Date	Amount of Dumped Material (Cubic Yards)	Remarks
1	1898-1911	110,700	Denny Regrade
	1928-1931	4,200,000	Denny Regrade
2	1976	114,000	Experimental PCB disposal site
3	197 - 1985	-	Four Mile Rock disposal site (contaminated sediments)
	1985-1987	-	Four Mile Rock disposal site (2 years of clean disposal)
4	1989-1990	130,000 (2)	PSDDA Disposal Site
5	1989	10,000	Ferry Terminal capping (4 acres)
6	1990	20,000	Denny Way Cap (3 acres)
7	1992	20,000	Pier 53-55 Cap (4.5 acres)
8	-	-	Piers 49-50 removed
9	-	-	Pier 71 removed
10	-	-	Piers 64-65 collapsed and removed
11	-	-	Pier 66 - Port renovation
12	-	-	Ship Yard
13	-	-	Ship Yard
14	-	-	New container dock (in 1979, dredging in face)
			(1) Data from P. Romberg, Metro, pers. comm., (1993)
			(2) Revelas et al., (1991)

TABLE 2A

Line statistics for mud samples

Definitions

1. R^2 = multiple correlation coefficient derived from the mean, sorting and skewness of each sample distribution along the line. This is a relative indication of how well the samples are related by transport.
2. **Case B:** Sediments becoming finer, better sorted and more negatively skewed in the direction of transport.
3. **Case C:** Sediments becoming coarser, better sorted and more positively skewed in the direction of transport.
4. N = number of possible pairs in the line of samples.
5. x = number of pairs making a particular trend in a specific direction.
6. Z = Z-score statistic: ** are those samples significant at the 99% level. * are those trends significant at the 95% level.
7. Status (i.e. net erosion, accretion or dynamic equilibrium) is determined by the shape of the X-distribution.
8. Directions are always "Down" the line of samples. (On Figures 4 and 15, line numbers are placed at the "Down" end of each line).

Line	Case R2	Direction	N	x	Z	Status
1m	B 1.00	UP	3	0	-0.65	Equilibrium
		DOWN	3	2	2.84**	
	C	UP	3	0	-0.65	
		DOWN	3	0	-0.65	
2m	B 1.00	UP	3	0	-0.65	Accretion
		DOWN	3	2	2.84**	
	C	UP	3	0	-0.65	
		DOWN	3	1	1.09	
3m	B 0.99	UP	10	2	0.72	Accretion
		DOWN	10	4	2.63**	
	C	UP	10	1	-0.24	
		DOWN	10	1	-0.24	
4m	B 0.74	UP	28	3	-0.29	Accretion
		DOWN	28	8	2.57**	
	C	UP	28	1	-1.43	
		DOWN	28	6	1.43	
5m	B 0.72	UP	28	3	-0.29	Accretion
		DOWN	28	12	4.86**	
	C	UP	28	1	-1.43	
		DOWN	28	6	1.43	
6m	B 0.62	UP	36	3	-0.76	Accretion
		DOWN	36	16	5.80**	
	C	UP	36	1	-1.76	
		DOWN	36	8	1.76*	
7m	B 0.69	UP	28	1	-1.43	Accretion
		DOWN	28	16	7.14**	
	C	UP	28	1	-1.43	
		DOWN	28	5	0.86	
8ma (duplicate)	B 0.59	UP	55	5	-0.76	Accretion
		DOWN	55	23	6.57**	
	C	UP	55	1	-2.40	
		DOWN	55	9	0.87	
8mb	B 0.92	UP	55	6	-0.36	Accretion
		DOWN	55	33	10.65**	
	C	UP	55	4	-1.17	
		DOWN	55	9	0.87	

Table ZA

Line	Case R2	Direction	N	x	Z	Status
9m	B 0.88	UP	55	2	-1.99	Mixed Case
		DOWN	55	30	9.43**	
	C	UP	55	4	-1.17	
		DOWN	55	15	3.31**	
10ma (duplicate)	B 0.89	UP	91	12	0.20	Accretion
		DOWN	91	50	12.24**	
	C	UP	91	6	-1.70	
		DOWN	91	14	0.83	
10mb	B 0.90	UP	91	13	0.52	Accretion
		DOWN	91	47	11.29**	
	C	UP	91	6	-1.70	
		DOWN	91	14	0.83	
11ma (duplicate)	B 0.78	UP	78	6	-1.28	Accretion
		DOWN	78	41	10.70**	
	C	UP	78	7	-0.94	
		DOWN	78	10	0.09	
11mb	B 0.87	UP	78	7	-0.94	Accretion
		DOWN	78	45	12.07**	
	C	UP	78	6	-1.28	
		DOWN	78	10	0.09	
12ma (duplicate)	B 0.81	UP	91	17	1.78*	Accretion
		DOWN	91	42	9.71**	
	C	UP	91	9	-0.75	
		DOWN	91	8	-1.07	
12mb	B 0.92	UP	91	12	0.20	Accretion
		DOWN	91	52	12.88**	
	C	UP	91	7	-1.39	
		DOWN	91	8	-1.07	
13ma (duplicate)	B 0.78	UP	120	12	-0.83	Accretion
		DOWN	120	58	11.87**	
	C	UP	120	14	-0.28	
		DOWN	120	16	0.28	
13mb	B 0.90	UP	120	17	0.55	Accretion
		DOWN	120	62	12.97**	
	C	UP	120	13	-0.55	
		DOWN	120	14	-0.28	

Table 2A

Line	Case R2	Direction	N	x	Z	Status
14ma (duplicate)	B 0.82	UP	120	15	0.00	Accretion
		DOWN	120	57	11.59**	
	C	UP	120	19	1.10	
		DOWN	120	9	-1.66	
14mb	B 0.78	UP	120	20	1.38	Accretion
		DOWN	120	53	10.49**	
	C	UP	120	14	-0.28	
		DOWN	120	19	1.10	
15ma (duplicate)	B 0.79	UP	120	10	-1.38	Accretion
		DOWN	120	55	11.04**	
	C	UP	120	18	0.83	
		DOWN	120	17	0.55	
15mb	B 0.85	UP	120	19	1.10	Accretion
		DOWN	120	51	9.94**	
	C	UP	120	13	-0.55	
		DOWN	120	20	1.38	
16ma (duplicate)	B 0.81	UP	120	11	-1.10	Accretion
		DOWN	120	56	11.32**	
	C	UP	120	18	0.83	
		DOWN	120	15	0.00	
16mb	B 0.85	UP	120	19	1.10	Accretion
		DOWN	120	54	10.77**	
	C	UP	120	13	-0.55	
		DOWN	120	20	1.38	
17ma (duplicate)	B 0.85	UP	136	13	-1.04	Accretion
		DOWN	136	73	14.52**	
	C	UP	136	21	1.04	
		DOWN	136	9	-2.07	
17mb	B 0.86	UP	136	21	1.04	Accretion
		DOWN	136	70	13.74**	
	C	UP	136	16	-0.26	
		DOWN	136	14	-0.78	
18ma (duplicate)	B 0.83	UP	136	22	1.30	Accretion
		DOWN	136	69	13.48**	
	C	UP	136	16	-0.26	
		DOWN	136	7	-2.59	

Line	Case R2	Direction	N	x	Z	Status
18mb	B 0.92	UP	136	22	1.30	Accretion
		DOWN	136	64	12.19**	
	C	UP	136	9	-2.07	
		DOWN	136	10	-1.81	
19ma (duplicate)	B 0.82	UP	153	19	-0.03	Accretion
		DOWN	153	74	13.41**	
	C	UP	153	12	-1.74	
		DOWN	153	23	0.95	
19mb	B 0.84	UP	153	22	0.70	Accretion
		DOWN	153	70	12.44**	
	C	UP	153	14	-1.25	
		DOWN	153	25	1.44	
20ma (duplicate)	B 0.78	UP	190	25	0.27	Accretion
		DOWN	190	87	13.87**	
	C	UP	190	25	0.27	
		DOWN	190	15	-1.92	
20mb	B 0.94	UP	190	28	0.93	Accretion
		DOWN	190	89	14.31**	
	C	UP	190	16	-1.70	
		DOWN	190	18	-1.26	
21ma (duplicate)	B 0.80	UP	276	44	1.73*	Accretion
		DOWN	276	108	13.38**	
	C	UP	276	43	1.55	
		DOWN	276	15	-3.55	
21mb	B 0.89	UP	276	40	1.00	Accretion
		DOWN	276	103	12.47**	
	C	UP	276	40	1.00	
		DOWN	276	19	-2.82	
22ma (duplicate)	B 0.84	UP	406	46	-0.71	Accretion
		DOWN	406	202	22.70**	
	C	UP	406	62	1.69*	
		DOWN	406	17	-5.06	
22mb	B 0.86	UP	406	45	-0.86	Accretion
		DOWN	406	198	22.10**	
	C	UP	406	52	0.19	
		DOWN	406	15	-5.36	

Line	Case R2	Direction	N	x	Z	Status
23ma (duplicate)	B 0.84	UP	435	41	-1.94	Deposition
		DOWN	435	240	26.91**	
	C	UP	435	55	0.09	
		DOWN	435	18	-5.27	
23mb	B 0.90	UP	435	50	-0.63	Deposition
		DOWN	435	235	26.19**	
	C	UP	435	46	-1.21	
		DOWN	435	18	-5.27	
24ma (duplicate)	B 0.79	UP	435	63	1.25	Deposition
		DOWN	435	234	26.04**	
	C	UP	435	43	-1.65	
		DOWN	435	16	-5.56	
24mb	B 0.76	UP	435	60	0.82	Deposition
		DOWN	435	214	23.14**	
	C	UP	435	70	2.27*	
		DOWN	435	37	-2.52	
25m (duplicate)	B 0.83	UP	406	65	2.14*	Deposition
		DOWN	406	178	19.10**	
	C	UP	406	62	1.69*	
		DOWN	406	17	-5.06	
25mb	B 0.72	UP	406	70	2.89**	Deposition
		DOWN	406	177	18.95**	
	C	UP	406	64	1.99*	
		DOWN	406	25	-3.86	
26ma (duplicate)	B 0.84	UP	300	50	2.18*	Accretion
		DOWN	300	95	10.04**	
	C	UP	300	25	-2.18	
		DOWN	300	40	0.44	
26mb	B 0.88	UP	300	56	3.23**	Accretion
		DOWN	300	97	10.39**	
	C	UP	300	28	-1.66	
		DOWN	300	45	1.31	
27m	B 0.91	UP	45	1	-2.08	Accretion
		DOWN	45	27	9.63**	
	C	UP	45	6	0.17	
		DOWN	45	2	-1.63	

Table ZA

Line	Case R2	Direction	N	x	Z	Status
28m	B 0.87	UP	55	2	-1.99	Accretion
		DOWN	55	37	12.28**	
	C	UP	55	3	-1.58	
		DOWN	55	3	-1.58	
29ma (duplicate)	B 0.85	UP	45	2	-1.63	Accretion
		DOWN	45	27	9.63**	
	C	UP	45	1	-2.08	
		DOWN	45	3	-1.18	
29mb	B 0.92	UP	45	2	-1.63	Accretion
		DOWN	45	31	11.44**	
	C	UP	45	1	-2.08	
		DOWN	45	2	-1.63	
30ma (duplicate)	B 0.74	UP	66	1	-2.70	Accretion
		DOWN	66	43	12.93**	
	C	UP	66	4	-1.58	
		DOWN	66	2	-2.33	
30mb	B 0.85	UP	66	3	-1.95	Accretion
		DOWN	66	48	14.79**	
	C	UP	66	0	-3.07	
		DOWN	66	7	-0.47	
31m	B 0.88	UP	66	12	1.40	Accretion
		DOWN	66	21	4.75**	
	C	UP	66	3	-1.95	
		DOWN	66	2	-2.33	
32m	B 0.98	UP	21	2	-0.41	Accretion
		DOWN	21	14	7.51**	
	C	UP	21	0	-1.73	
		DOWN	21	1	-1.07	
33ma (duplicate)	B 0.98	UP	45	4	-0.73	Accretion
		DOWN	45	31	11.44**	
	C	UP	45	3	-1.18	
		DOWN	45	5	-0.28	
33mb	B 0.95	UP	45	3	-1.18	Accretion
		DOWN	45	31	11.44**	
	C	UP	45	4	-0.73	
		DOWN	45	3	-1.18	

Line	Case R2	Direction	N	x	Z	Status
34ma (duplicate)	B 0.98	UP	66	4	-1.58	Accretion
		DOWN	66	42	12.56**	
	C	UP	66	7	-0.47	
		DOWN	66	10	0.65	
34mb	B 0.96	UP	66	4	-1.58	Accretion
		DOWN	66	42	12.56**	
	C	UP	66	5	-1.21	
		DOWN	66	9	0.28	
35m	B 0.99	UP	66	10	0.65	Accretion
		DOWN	66	32	8.84**	
	C	UP	66	9	0.28	
		DOWN	66	10	0.65	
36ma (duplicate)	B 0.97	UP	21	2	-0.41	Deposition
		DOWN	21	7	2.89**	
	C	UP	21	2	-0.41	
		DOWN	21	6	2.23*	
36mb	B 0.95	UP	21	3	0.25	Deposition
		DOWN	21	9	4.21**	
	C	UP	21	2	-0.41	
		DOWN	21	4	0.91	
37m	B 0.88	UP	21	3	0.25	Equilibrium
		DOWN	21	5	1.57	
	C	UP	21	2	-0.41	
		DOWN	21	8	3.55**	
38ma (duplicate)	B 0.60	UP	15	1	-0.68	Equilibrium
		DOWN	15	4	1.66*	
	C	UP	15	1	-0.68	
		DOWN	15	5	2.44**	
38mb	B 0.94	UP	15	1	-0.68	Equilibrium
		DOWN	15	1	-0.68	
	C	UP	15	2	0.10	
		DOWN	15	10	6.34**	
39m	B 0.54	UP	36	3	-0.76	Deposition
		DOWN	36	12	3.78**	
	C	UP	36	1	-1.76	
		DOWN	36	7	1.26	

Line	Case R2	Direction	N	x	Z	Status
40ma (duplicate)	B 0.99	UP	28	2	-0.86	Equilibrium
		DOWN	28	4	0.29	
	C	UP	28	3	-0.29	
		DOWN	28	15	6.57**	
40mb	B 0.94	UP	28	2	-0.86	Equilibrium
		DOWN	28	4	0.29	
	C	UP	28	5	0.86	
		DOWN	28	16	7.14**	
41ma (duplicate)	B 0.88	UP	28	2	-0.86	Accretion
		DOWN	28	9	3.14**	
	C	UP	28	3	-0.29	
		DOWN	28	5	0.86	
41mb	B 0.89	UP	28	2	-0.86	Accretion
		DOWN	28	12	4.86**	
	C	UP	28	3	-0.29	
		DOWN	28	5	0.86	
42m	B 0.79	UP	36	6	0.76	Accretion
		DOWN	36	14	4.79**	
	C	UP	36	3	-0.76	
		DOWN	36	2	-1.26	
43m	B 0.97	UP	120	20	1.38	Accretion
		DOWN	120	64	13.53**	
	C	UP	120	22	1.93*	
		DOWN	120	1	-3.86	
44m	B 0.91	UP	190	20	-0.82	Accretion
		DOWN	190	105	17.82**	
	C	UP	190	12	-2.58	
		DOWN	190	3	-4.55	
45m	B 0.91	UP	190	8	-3.45	Accretion
		DOWN	190	102	17.17**	
	C	UP	190	22	-0.38	
		DOWN	190	2	-4.77	
46m	B 0.90	UP	171	6	-3.56	Accretion
		DOWN	171	97	17.49**	
	C	UP	171	12	-2.17	
		DOWN	171	4	-4.02	

Line	Case R2	Direction	N	x	Z	Status
47m	B 0.91	UP	120	5	-2.76	Accretion
		DOWN	120	78	17.39**	
	C	UP	120	10	-1.38	
		DOWN	120	1	-3.86	
48m	B 0.94	UP	136	5	-3.11	Accretion
		DOWN	136	88	18.41**	
	C	UP	136	13	-1.04	
		DOWN	136	2	-3.89	
49m	B 0.87	UP	210	6	-4.23	Accretion
		DOWN	210	118	19.14**	
	C	UP	210	14	-2.56	
		DOWN	210	5	-4.43	
50m	B 0.89	UP	231	5	-4.75	Accretion
		DOWN	231	117	17.53**	
	C	UP	231	17	-2.36	
		DOWN	231	8	-4.15	
51m	B 0.83	UP	171	4	-4.02	Accretion
		DOWN	171	97	17.49**	
	C	UP	171	7	-3.32	
		DOWN	171	5	-3.79	
52m	B 0.85	UP	171	5	-3.79	Accretion
		DOWN	171	95	17.02**	
	C	UP	171	5	-3.79	
		DOWN	171	14	-1.71	
53ma (duplicate)	B 0.84	UP	171	8	-3.09	Accretion
		DOWN	171	97	17.49**	
	C	UP	171	4	-4.02	
		DOWN	171	6	-3.56	
53mb	B 0.79	UP	171	8	-3.09	Accretion
		DOWN	171	97	17.49**	
	C	UP	171	6	-3.56	
		DOWN	171	6	-3.56	
54ma (duplicate)	B 0.87	UP	210	7	-4.02	Accretion
		DOWN	210	125	20.60**	
	C	UP	210	14	-2.56	
		DOWN	210	2	-5.06	

Line	Case R2	Direction	N	x	Z	Status
54mb	B 0.80	UP	210	9	-3.60	Accretion
		DOWN	210	130	21.65**	
	C	UP	210	12	-2.97	
		DOWN	210	0	-5.48	
55ma (duplicate)	B 0.82	UP	153	6	-3.21	Accretion
		DOWN	153	91	17.57**	
	C	UP	153	4	-3.70	
		DOWN	153	3	-3.94	
55mb	B 0.96	UP	153	12	-1.74	Accretion
		DOWN	153	100	19.77**	
	C	UP	153	8	-2.72	
		DOWN	153	4	-3.70	
56m	B 0.86	UP	171	5	-3.79	Accretion
		DOWN	171	100	18.18**	
	C	UP	171	4	-4.02	
		DOWN	171	5	-3.79	
57m	B 0.91	UP	153	5	-3.45	Accretion
		DOWN	153	85	16.10**	
	C	UP	153	8	-2.72	
		DOWN	153	4	-3.70	
58m	B 0.86	UP	120	2	-3.59	Accretion
		DOWN	120	75	16.56**	
	C	UP	120	5	-2.76	
		DOWN	120	4	-3.04	
58m	B 0.89	UP	136	5	-3.11	Accretion
		DOWN	136	72	14.26**	
	C	UP	136	11	-1.56	
		DOWN	136	4	-3.37	
60m	B 0.85	UP	136	4	-3.37	Accretion
		DOWN	136	81	16.59**	
	C	UP	136	4	-3.37	
		DOWN	136	5	-3.11	
61m	B 0.84	UP	153	5	-3.45	Accretion
		DOWN	153	88	16.84**	
	C	UP	153	6	-3.21	
		DOWN	153	3	-3.94	

Table 2A

Line	Case R2	Direction	N	x	Z	Status
62ma (duplicate)	B 0.87	UP	105	2	-3.28	Accretion
		DOWN	105	69	16.49**	
	C	UP	105	4	-2.69	
		DOWN	105	3	-2.99	
62mb	B 0.98	UP	105	3	-2.99	Accretion
		DOWN	105	76	18.55**	
	C	UP	105	3	-2.99	
		DOWN	105	5	-2.40	
63ma (duplicate)	B 0.89	UP	105	2	-3.28	Accretion
		DOWN	105	68	16.19**	
	C	UP	105	5	-2.40	
		DOWN	105	3	-2.99	
63mb	B 0.96	UP	105	3	-2.99	Accretion
		DOWN	105	77	18.85**	
	C	UP	105	4	-2.69	
		DOWN	105	5	-2.40	
64ma (duplicate)	B 0.89	UP	91	1	-3.29	Accretion
		DOWN	91	62	16.05**	
	C	UP	91	5	-2.02	
		DOWN	91	4	-2.34	
64mb	B 0.99	UP	91	11	-0.12	Accretion
		DOWN	91	70	18.58**	
	C	UP	91	3	-2.65	
		DOWN	91	4	-2.34	
65ma (duplicate)	B 0.84	UP	78	2	-2.65	Accretion
		DOWN	78	53	14.81**	
	C	UP	78	4	-1.97	
		DOWN	78	2	-2.65	
65mb	B 0.95	UP	78	3	-2.31	Accretion
		DOWN	78	56	15.83**	
	C	UP	78	3	-2.31	
		DOWN	78	4	-1.97	
66ma (duplicate)	B 0.85	UP	91	4	-2.34	Accretion
		DOWN	91	60	15.41**	
	C	UP	91	7	-1.39	
		DOWN	91	5	-2.02	

Table ZA

Line	Case R2	Direction	N	x	Z	Status
66mb	B 0.97.	UP	91	5	-2.02	Accretion
		DOWN	91	66	17.31**	
	C	UP	91	6	-1.70	
		DOWN	91	8	-1.07	
67ma (duplicate)	B 0.82	UP	91	1	-3.29	Accretion
		DOWN	91	62	16.05**	
	C	UP	91	7	-1.39	
		DOWN	91	3	-2.65	
67mb	B 0.96	UP	91	3	-2.65	Accretion
		DOWN	91	66	17.31**	
	C	UP	91	6	-1.70	
		DOWN	91	6	-1.70	
68ma (duplicate)	B 0.93	UP	78	0	-3.34	Accretion
		DOWN	78	50	13.78**	
	C	UP	78	11	0.43	
		DOWN	78	2	-2.65	
68mb	B 0.98	UP	78	2	-2.65	Accretion
		DOWN	78	55	15.49**	
	C	UP	78	10	0.09	
		DOWN	78	4	-1.97	
69ma (duplicate)	B 0.93	UP	66	0	-3.07	Accretion
		DOWN	66	46	14.05**	
	C	UP	66	9	0.28	
		DOWN	66	2	-2.33	
69mb	B 0.93	UP	66	0	-3.07	Accretion
		DOWN	66	49	15.17**	
	C	UP	66	6	-0.84	
		DOWN	66	4	-1.58	
70ma (duplicate)	B 0.99	UP	66	0	-3.07	Accretion
		DOWN	66	50	15.54**	
	C	UP	66	7	-0.47	
		DOWN	66	4	-1.58	
70mb	B 0.99	UP	66	0	-3.07	Accretion
		DOWN	66	51	15.91**	
	C	UP	66	6	-0.84	
		DOWN	66	4	-1.58	

TABLE ZA

Line	Case R2	Direction	N	x	Z	Status
71ma (duplicate)	B 0.99	UP	66	1	-2.70	Accretion
		DOWN	66	50	15.54**	
	C	UP	66	4	-1.58	
		DOWN	66	5	-1.21	
71mb	B 0.99	UP	66	1	-2.70	Accretion
		DOWN	66	50	15.54**	
	C	UP	66	4	-1.58	
		DOWN	66	5	-1.21	
72ma (duplicate)	B 0.98	UP	66	0	-3.07	Accretion
		DOWN	66	48	14.79**	
	C	UP	66	4	-1.58	
		DOWN	66	2	-2.33	
72mb	B 0.98	UP	66	0	-3.07	Accretion
		DOWN	66	48	14.79**	
	C	UP	66	4	-1.58	
		DOWN	66	2	-2.33	
73ma (duplicate)	B 0.97	UP	36	0	-2.27	Accretion
		DOWN	36	27	11.34**	
	C	UP	36	4	-0.25	
		DOWN	36	3	-0.76	
73mb	B 0.94	UP	36	0	-2.27	Accretion
		DOWN	36	27	11.34**	
	C	UP	36	4	-0.25	
		DOWN	36	1	-1.76	
74ma (duplicate)	B 0.96	UP	55	5	-0.76	Accretion
		DOWN	55	31	9.84**	
	C	UP	55	5	-0.76	
		DOWN	55	2	-1.99	
74mb	B 0.94	UP	55	4	-1.17	Accretion
		DOWN	55	32	10.24**	
	C	UP	55	5	-0.76	
		DOWN	55	3	-1.58	
75ma (duplicate)	B 0.87	UP	21	2	-0.41	Accretion
		DOWN	21	10	4.87**	
	C	UP	21	0	-1.73	
		DOWN	21	4	0.91	

Line	Case R2	Direction	N	x	Z	Status
75mb	B 0.90	UP	21	0	-1.73	Accretion
		DOWN	21	10	4.87**	
	C	UP	21	2	-0.41	
		DOWN	21	2	-0.41	
76ma (duplicate)	B 0.89	UP	55	4	-1.17	Deposition
		DOWN	55	31	9.84**	
	C	UP	55	9	0.87	
		DOWN	55	3	-1.58	
76mb	B 0.91	UP	55	4	-1.17	Deposition
		DOWN	55	32	10.24**	
	C	UP	55	9	0.87	
		DOWN	55	3	-1.58	
77m (duplicate)	B 0.87	UP	66	10	0.65	Deposition
		DOWN	66	33	9.21**	
	C	UP	66	11	1.02	
		DOWN	66	3	-1.95	
77mb	B 0.89	UP	66	9	0.28	Deposition
		DOWN	66	33	9.21**	
	C	UP	66	11	1.02	
		DOWN	66	3	-1.95	
78ma (duplicate)	B 0.87	UP	36	5	0.25	Deposition
		DOWN	36	17	6.30**	
	C	UP	36	6	0.76	
		DOWN	36	3	-0.76	
78mb	B 0.84	UP	36	7	1.26	Deposition
		DOWN	36	16	5.80**	
	C	UP	36	3	-0.76	
		DOWN	36	4	-0.25	
79m	B 0.65	UP	21	0	-1.73	Accretion
		DOWN	21	13	6.85**	
	C	UP	21	1	-1.07	
		DOWN	21	3	0.25	
80m	B 0.87	UP	91	14	0.83	Mixed Case
		DOWN	91	19	2.42**	
	C	UP	91	2	-2.97	
		DOWN	91	42	9.71**	

Table 2A

Line	Case R2	Direction	N	x	Z	Status
81m	B 0.88	UP	120	15	0.00	?
		DOWN	120	18	0.83	
	C	UP	120	2	-3.59	
		DOWN	120	71	15.46**	

TABLE 2B

Line statistics for sand samples

Definitions

1. R^2 = multiple correlation coefficient derived from the mean, sorting and skewness of each sample distribution along the line. This is a relative indication of how well the samples are related by transport.
2. **Case B**: Sediments becoming finer, better sorted and more negatively skewed in the direction of transport.
3. **Case C**: Sediments becoming coarser, better sorted and more positively skewed in the direction of transport.
4. **N** = number of possible pairs in the line of samples.
5. **x** = number of pairs making a particular trend in a specific direction.
6. **Z** = Z-score statistic: ** are those samples significant at the 99% level. * are those trends significant at the 95% level.
7. Status (i.e. net erosion, accretion or dynamic equilibrium) is determined by the shape of the X-distribution.
8. Directions are always "Down" the line of samples. (On Figures 4 and 15, line numbers are placed at the "Down" end of each line).

Table 2B

Line	Case R2	Direction	N	x	Z	Status
1s	B 0.90	UP	21	2	-0.41	Erosion
		DOWN	21	0	-1.73	
	C	UP	21	1	-1.07	
		DOWN	21	9	4.21**	
2s	B 0.74	UP	28	1	-1.43	Equilibrium
		DOWN	28	1	-1.43	
	C	UP	28	4	0.29	
		DOWN	28	13	5.43**	
3s	B 0.66	UP	28	4	0.29	Equilibrium
		DOWN	28	1	-1.43	
	C	UP	28	6	1.43	
		DOWN	28	13	5.43**	
4s	B 0.96	UP	15	0	-1.46	Equilibrium
		DOWN	15	0	-1.46	
	C	UP	15	1	-0.68	
		DOWN	15	5	2.44**	
5s	B 0.98	UP	15	0	-1.46	Equilibrium
		DOWN	15	0	-1.46	
	C	UP	15	1	-0.68	
		DOWN	15	5	2.44**	
6s	B 0.70	UP	55	3	-1.58	Equilibrium
		DOWN	55	15	3.31**	
	C	UP	55	9	0.87	
		DOWN	55	7	0.05	
7s	B 1.00	UP	3	0	-0.65	Equilibrium
		DOWN	3	0	-0.65	
	C	UP	3	0	-0.65	
		DOWN	3	3	4.58**	
8sa (duplicate)	B 0.98	UP	66	7	-0.47	?
		DOWN	66	7	-0.47	
	C	UP	66	13	1.77*	
		DOWN	66	30	8.10**	
8sb	B 0.98	UP	66	2	-2.33	?
		DOWN	66	8	-0.09	
	C	UP	66	14	2.14*	
		DOWN	66	33	9.21**	

Line	Case R2	Direction	N	x	z	Status
9sa (duplicate)	B 0.96	UP	66	7	-0.47	?
		DOWN	66	8	-0.09	
	C	UP	66	11	1.02	
		DOWN	66	24	5.86**	
9sb	B 0.98	UP	66	2	-2.33	?
		DOWN	66	11	1.02	
	C	UP	66	11	1.02	
		DOWN	66	28	7.35**	
10s	B 0.97	UP	55	1	-2.40	Mixed Case
		DOWN	55	15	3.31**	
	C	UP	55	7	0.05	
		DOWN	55	29	9.02**	
11s	B 0.97	UP	55	1	-2.40	?
		DOWN	55	11	1.68*	
	C	UP	55	7	0.05	
		DOWN	55	33	10.65**	
12s	B 0.98	UP	45	1	-2.08	?
		DOWN	45	9	1.52	
	C	UP	45	5	-0.28	
		DOWN	45	25	8.73**	
13s	B 0.96	UP	55	6	-0.36	Mixed Case
		DOWN	55	13	2.50**	
	C	UP	55	8	0.46	
		DOWN	55	24	6.98**	
14s	B 0.96	UP	55	1	-2.40	Mixed Case
		DOWN	55	15	3.31**	
	C	UP	55	6	-0.36	
		DOWN	55	29	9.02**	
15sa (duplicate)	B 0.96	UP	66	2	-2.33	Mixed Case
		DOWN	66	16	2.88**	
	C	UP	66	8	-0.09	
		DOWN	66	35	9.96**	
15sb	B 0.96	UP	66	3	-1.95	Mixed Case
		DOWN	66	23	5.49**	
	C	UP	66	7	-0.47	
		DOWN	66	26	6.61**	

Line	Case R2	Direction	N	x	Z	Status
16s	B 0.96	UP	66	2	-2.33	Mixed Case
		DOWN	66	17	3.26**	
	C	UP	66	7	-0.47	
		DOWN	66	35	9.96**	
17s	B 0.96	UP	55	1	-2.40	Mixed Case
		DOWN	55	14	2.90**	
	C	UP	55	6	-0.36	
		DOWN	55	29	9.02**	
18s	B 0.95	UP	66	4	-1.58	Mixed Case
		DOWN	66	16	2.88**	
	C	UP	66	12	1.40	
		DOWN	66	28	7.35**	
19s	B 0.82	UP	10	0	-1.20	Equilibrium
		DOWN	10	2	0.72	
	C	UP	10	2	0.72	
		DOWN	10	4	2.63**	
20s	B 0.97	UP	28	7	2.00*	Erosion
		DOWN	28	4	0.29	
	C	UP	28	1	-1.43	
		DOWN	28	14	6.00**	
21sa (duplicate)	B 0.98	UP	36	7	1.26	Equilibrium
		DOWN	36	4	-0.25	
	C	UP	36	0	-2.27	
		DOWN	36	24	9.83**	
21sb	B 0.96	UP	36	8	1.76*	Equilibrium
		DOWN	36	0	-2.27	
	C	UP	36	4	-0.25	
		DOWN	36	22	8.82**	
22sa (duplicate)	B 0.93	UP	55	11	1.68*	Erosion
		DOWN	55	12	2.09*	
	C	UP	55	2	-1.99	
		DOWN	55	26	7.80**	
22sb	B 0.97	UP	55	9	0.87	Erosion
		DOWN	55	3	-1.58	
	C	UP	55	10	1.27	
		DOWN	55	33	10.65**	

Line	Case R2	Direction	N	x	Z	Status
23sa (duplicate)	B 0.92	UP	91	15	1.15	Equilibrium
		DOWN	91	7	-1.39	
	C	UP	91	11	-0.12	
		DOWN	91	51	12.56**	
23sb	B 0.93	UP	91	11	-0.12	Equilibrium
		DOWN	91	4	-2.34	
	C	UP	91	15	1.15	
		DOWN	91	55	13.83**	
24s	B 0.92	UP	120	15	0.00	Equilibrium
		DOWN	120	14	-0.28	
	C	UP	120	8	-1.93	
		DOWN	120	72	15.73**	
25s	B 0.89	UP	120	7	-2.21	Mixed Case
		DOWN	120	26	3.04**	
	C	UP	120	6	-2.48	
		DOWN	120	64	13.53**	
26sa (duplicate)	B 0.86	UP	190	14	-2.14	Equilibrium
		DOWN	190	29	1.15	
	C	UP	190	21	-0.60	
		DOWN	190	104	17.60**	
26sb	B 0.92	UP	190	12	-2.58	Equilibrium
		DOWN	190	28	0.93	
	C	UP	190	29	1.15	
		DOWN	190	106	18.04**	
27s	B 1.00	UP	3	0	-0.65	Erosion
		DOWN	3	0	-0.65	
	C	UP	3	0	-0.65	
		DOWN	3	3	4.58**	
28s	B 1.00	UP	3	0	-0.65	Accretion
		DOWN	3	0	-0.65	
	C	UP	3	0	-0.65	
		DOWN	3	2	2.84**	
29s	B 0.99	UP	10	1	-0.24	Equilibrium
		DOWN	10	2	0.72	
	C	UP	10	1	-0.24	
		DOWN	10	4	2.63**	

TABLE 3A

SUMMARY OF THE SEDIMENT TRANSPORT ENVIRONMENTS IN ELLIOTT BAY AND THE DUWAMISH RIVER (MUD)

Environment	Lines	No. of Sample Lines	R2 Values		Interpretation of the X-Distribution
			Mean	S.D.	
1	Seattle Waterfront 1 to 26	26	0.81	0.10	Net accretion (Figs.6-8)
2	Seattle Nearshore 27 to 32	6	0.87	0.08	Net accretion (Fig.9)
3	Harbor Island 33 to 42	10	0.86	0.17	Dominantly Net accretion (Figs.10-12)
4	Central Elliott Bay 43 to 74	32	0.89	0.05	Net accretion (Fig.13)
5	Georgetown Reach 75 to 78	4	0.88	0.01	Total deposition (Fig.14)
6	Upper Duwamish River 79 to 81	3	0.80	0.13	?

TABLE 3B

SUMMARY OF THE SEDIMENT TRANSPORT ENVIRONMENTS IN ELLIOTT BAY AND THE DUWAMISH RIVER (SAND)

Environment	Lines	No. of Sample Lines	R2 Values		Interpretation of the X-Distribution
			Mean	S.D.	
1	Magnolia Bluff 1 to 7, 19	8	0.85	0.14	Dynamic Equilibrium (Figs.17 and 18)
2	Harbor Island 8 to 18	11	0.96	0.01	Mixed Case
3	Duwamish Head 20 to 26	7	0.92	0.04	Dynamic Equilibrium
4	PSDDA Disposal Site 27 to 28	2	1.00	-	?
5	Harbor Island Reach 29	1	0.99	-	Dynamic Equilibrium

APPENDIX I

Sediment Transport Model

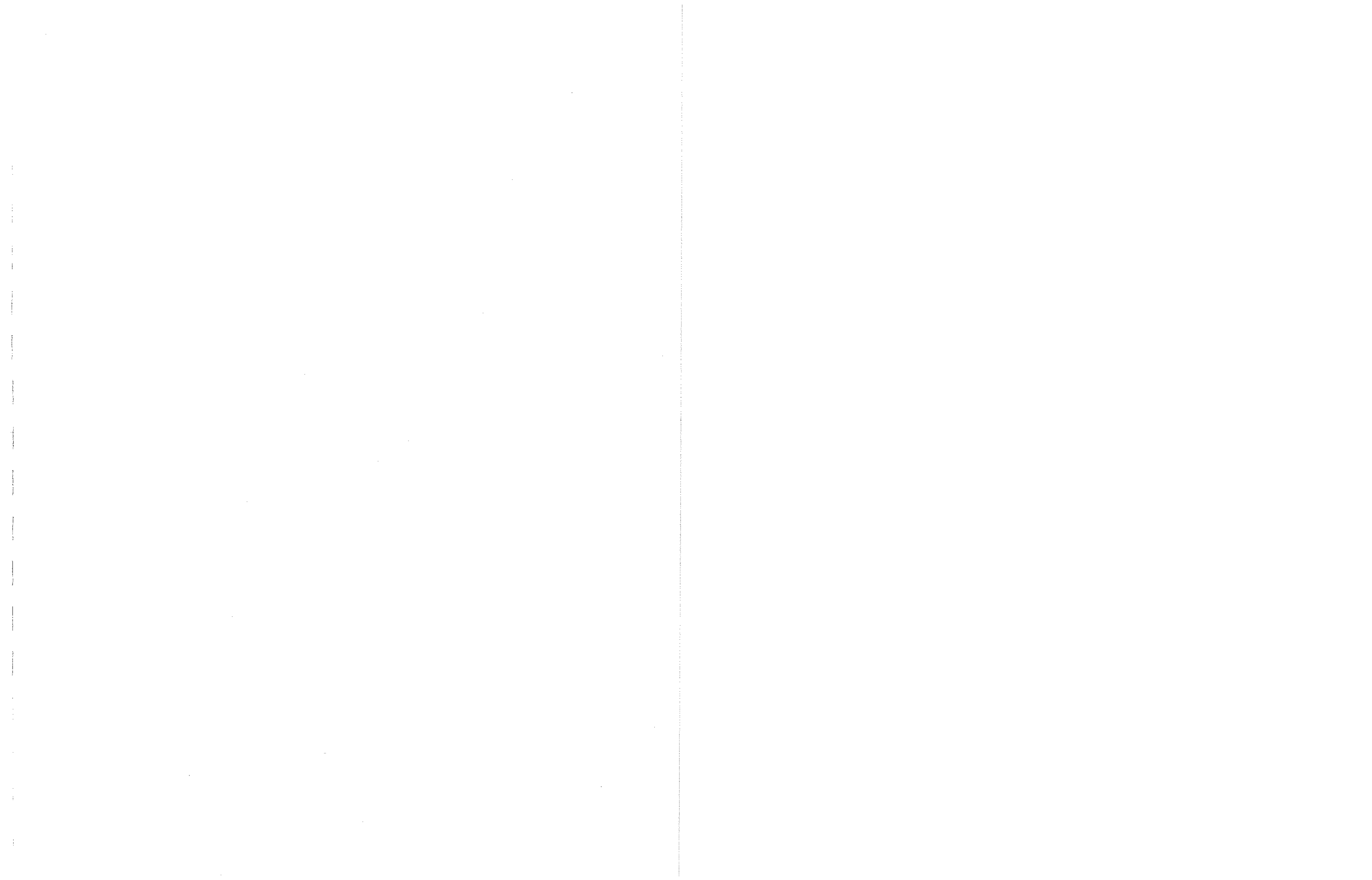


TABLE OF CONTENTS

- 1.0 SEDIMENT TRANSPORT MODEL
 - 1.1 Case A (development of a lag deposit)
 - 1.2 Case B (sediment becoming finer in the direction of transport)
 - 1.3 Case C (sediment becoming coarser in the direction of transport)
- 2.0 METHOD TO DETERMINE TRANSPORT DIRECTION FROM GRAIN-SIZE DISTRIBUTIONS
- 3.0 INTERPRETATION OF THE X-DISTRIBUTION

LIST OF FIGURES

- Figure A -1: Sediment transport model to develop a lag deposit.
- Figure A -2: Diagram showing the extremes in shape of transport functions $t(s)$.
- Figure A -3: Sediment transport model relating deposits in the direction of transport.
- Figure A -4: Summary diagram of t_1 and t_2 and corresponding X-distributions for Cases B and C.
- Figure A -5: Summary of the interpretations given to the shapes of X-distributions relative to the D_1 and D_2 deposits.

LIST OF TABLES

- Table A -1: Summary of the sediment transport interpretations when one deposit is compared to another.

1.0 SEDIMENT TRANSPORT MODEL

The following is a brief review of the transport model, a detailed analysis of which is contained in McLaren and Bowles (1985).

1.1 Case A (development of a lag deposit)

Consider a sedimentary deposit which has a grain-size distribution denoted by the function $g(s)$ (Fig. A -1). where 's' is grain size in phi units. If eroded, the sediment that goes into transport has a new distribution, $r(s)$, which is derived from $g(s)$ according to the function $t(s)$ so that:

$$r(s_i) = kg(s_i) t(s_i) \quad (1)$$

or
$$t(s_i) = \frac{r(s_i)}{kg(s_i)}$$

where $g(s_i)$ and $r(s_i)$ define the proportion of the sediment in the i^{th} grain-size class interval for each of the sediment distributions.

k is a scaling factor that normalizes $r(s)$ so that:

$$\sum_{i=1}^N r s_i = 1$$

thus
$$k = \frac{1}{\sum_{i=1}^N g(s_i) t(s_i)}$$

With the removal of $r(s)$ from $g(s)$ the remaining sediment (a lag) has a new distribution denoted by $d(s)$ (Fig. A -1) where :

$$d(s_i) = kg(s_i)[1 - t(s_i)]$$

or
$$t'(s_i) = \frac{d(s_i)}{k'g(s_i)}$$

where
$$t'(s_i) = 1 - t(s_i)$$

and
$$k' = \frac{1}{\sum_{i=1}^N g(s_i)[1 - t(s_i)]}$$

The function, $t(s)$, is defined as a sediment transfer function and is described in exactly the same manner as a grain-size distribution function. It may be thought of as a

function that incorporates all sedimentary and dynamic processes that result in initial movement and transport of particular grain sizes during a unit of time.

Data from flume experiments show that distributions of transfer functions change from having a high negative skewness to being nearly symmetrical (although still negatively skewed) as the energy of the eroding/transporting process increases. These two extremes in shape are termed low energy and high energy transfer functions respectively (Fig. A -2). The shape of $t(s)$ is also dependent, not only on changing energy levels of the process involved in erosion and transport, but also on the initial distribution of $g(s)$ (Fig. A -1). The coarser $g(s)$ is, the less likely it is to be acted upon by a high energy transfer function. Conversely, the finer $g(s)$ is, the easier it becomes for a high energy transfer function to operate on it. In other words, the same process may be represented by a high energy transfer function when acting on fine sediments, and by a low energy transfer function when acting on coarse sediments. The terms, high and low energy are, therefore, relative to the distribution of $g(s)$.

The fact that $t(s)$ appears to be mainly a negatively skewed function results in $r(s)$, the sediment in transport, always becoming finer and more negatively skewed than $g(s)$ (Fig. A -1). The function $1 - t(s)$ is, therefore, positively skewed, with the result that $d(s)$, the lag remaining after $r(s)$ has been removed, will always be coarser and more positively skewed than the original source sediment.

If $t(s)$ is applied to $g(s)$ an infinite number of times (i.e. 'n' times), then the variance of both $g(s)$ and $d(s)$ will approach zero (i.e. sorting will become better). However, depending on the initial distribution of $g(s)$, it is possible for variance to become greater before eventually decreasing. Because the phi scale produces approximately Gaussian or normal distributions which are symmetrical, it is probable that an increasing variance will rarely be observed.

Given two sediments, $d_1(s)$ and $d_2(s)$, and $d_2(s)$ is coarser, better sorted and more positively skewed than $d_1(s)$, it may be possible to conclude that $d_2(s)$ is a lag of $d_1(s)$ and that the two distributions were originally similar (Case A; Table A -1).

1.2 Case B (Sediments becoming finer in the direction of transport)

Consider a sequence of deposits [$d_1(s)$, $d_2(s)$, $d_3(s)$] that follows the direction of the sediment in transport (Fig. A -3). Each deposit is derived from its corresponding sediment in transport, and according to the '3-box' model shown in Figure A -1, each $d_n(s)$ can be considered a lag of each $r_n(s)$. Thus $d_n(s)$ will be coarser, better sorted and more positively skewed than $r_n(s)$. Similarly, each $r_n(s)$ is acted upon by its corresponding $t_n(s)$ with the result that the sediment in transport becomes progressively finer, better sorted and more negatively skewed.

Any two sequential deposits [e.g. $d_1(s)$ and $d_2(s)$] may be related to each other by a function $X(s)$ so that :

$$d_2(s) = kd_1(s)X(s)$$

$$\text{where } k = \frac{1}{\sum_{i=1}^N d_1(s_i)X(s_i)}$$

$$\text{or } X(s) = \frac{d_2(s)}{kd_1(s)}$$

As illustrated in Figure A-3, $d_2(s)$ can also be related to $d_1(s)$ by:

$$d_2(s) = \frac{kd_1(s)t_1(s)[1-t_2(s)]}{1-t_1(s)} \\ = kd_1(s)X(s) \quad (2)$$

$$\text{where } X(s) = \frac{t_1(s)[1-t_2(s)]}{1-t_1(s)} \quad (3)$$

The function $X(s)$ combines the effects of two transfer functions $t_1(s)$ and $t_2(s)$ (Equation 3). It may also be considered as a transfer function in that it provides the statistical relationship between the two deposits and it incorporates all of the processes responsible for sediment erosion, transport and deposition over the period of time represented by the samples. The deposit $d_2(s)$ will, therefore, change relative to $d_1(s)$ in accordance to the shape of $X(s)$ which, in turn, is derived from the combination of $t_1(s)$ and $t_2(s)$ as expressed in Equation 3. It is important to note that $X(s)$ can be derived from the deposits themselves (Equation 2) and it provides the relative probability of any particular sized grain being moved.

Using empirically derived $t(s)$ functions it can be shown that when energy is decreasing in the direction of transport [i.e. $t_2(s) < t_1(s)$] and both are low energy functions (Fig A-4), then $X(s)$ is always a negatively skewed distribution. This will result in $d_2(s)$ becoming finer, better sorted and more negatively skewed than $d_1(s)$. Therefore, given two sediments, $d_1(s)$ and $d_2(s)$ and $d_2(s)$ is finer, better sorted and more negatively skewed than $d_1(s)$, it may be possible to conclude that the direction of sediment transport is from d_1 to d_2 (Table A -1).

1.3 Case C (Sediments becoming coarser in the direction of transport)

In the event that $t_1(s)$ is a high energy function (Fig. A-2), and $t_2(s) < t_1(s)$ (i.e. energy is decreasing in the direction of transport), the result of Equation 3 will produce a positively skewed $X(s)$ distribution (Fig. A-4). Therefore, $d_2(s)$ will become coarser, better sorted and more positively skewed than $d_1(s)$ in the direction of transport, and should this relationship be observed, it may be possible to conclude that the direction of sediment transport is from d_1 to d_2 (Table A -1).

It is interesting to note that sediments cannot become coarser forever, because, with coarsening it becomes less and less likely that the transport processes will maintain high energy characteristics. As the deposits become coarser, the transfer function describing the processes will revert to a low energy function with the result that the sediment must become finer again.

Cases A and C produce identical grain-size changes between d_1 and d_2 (Table A-1). Generally, however, the geological interpretation of the environments being sampled will clearly differentiate between the two Cases.

2.0 METHOD TO DETERMINE TRANSPORT DIRECTION FROM GRAIN-SIZE DISTRIBUTIONS

Clearly the model presented above does not result in perfect sequential changes of grain-size distributions in the direction of sediment transport, although numerous authors have recognized general changes in specific parameters (e.g. mean grain size or sorting). The model demands specific changes in all three parameters (mean, sorting

and skewness) to suggest a transport direction. Given such complicating factors as variability in 'original source', probable local and temporal variability in the transfer functions, and variable time intervals represented by the samples themselves, it is not surprising that sequential changes in grain-size distributions are seldom recognized.

One approach that appears to be successful in recognizing trends is a simple statistical method whereby the Case (Table A -1) is determined among all possible pairs in a sample sequence. Given a sequence of 'n' samples, there are $\frac{n^2-n}{2}$ directionally-orientated pairs that may exhibit a transport trend in one direction, and an equal number of pairs in the opposite direction. When any two samples are compared with respect to their mean size, sorting and skewness, 8 possible trends exist; compared to d_1, d_2 may be: (i) finer (F), better sorted (B) and more negatively skewed (-); (ii) coarser (C), more poorly sorted (P) and more positively skewed (+); (iii) C, B, -; (iv) F, P, -; (v) C, P, -; (vi) F, B, +; (vii) C, B, +; or (viii) F, P +. Of these trends, only two are of interest, namely F, B, - (Case B) and C, B, + (Case A or C), for which there is a 1/8 probability of either occurring at random ($p = 0.125$). To determine if the number of occurrences that a particular Case exceeds the random probability of 0.125 the following two hypotheses are tested :

H_0 : $p < 0.125$ and there is no preferred direction; and

H_1 : $p > 0.125$ and transport is occurring in a preferred direction.

Using the Z-score in a one-tailed test, H_1 is accepted if:

$$Z = \frac{x - Np}{\sqrt{Npq}} > 1.645 \text{ (0.05 level of significance)}$$

or

$$> 2.33 \text{ (0.01 level of significance)}$$

where: x = observed number of pairs representing a particular Case in one of the two opposing directions; N = total number of possible unidirectional pairs.

$$N = \frac{n^2 - n}{2} \text{ where } n = \text{number of samples in sequence}$$

$$p = 0.125; \text{ and}$$

$$q = 1.0 - p = 0.875$$

The Z statistic is considered valid for $N > 30$ (i.e. a large sample). Thus, for this application, a suite of 8 or 9 samples is the minimum required to evaluate adequately a transport direction

$$\text{ie. } \frac{9^2 - 9}{2} = 36 \text{ (the total possible pairs in one direction)}$$

3.0 INTERPRETATION OF THE X-DISTRIBUTION

Empirical examination of X-distributions from a large number of different environments has shown that there are four basic shapes that the distributions can take relative to the distributions of D_1 and D_2 deposits (Fig. A -5). These are as follows:

- (1) The shape of the X-distribution resembles the D_1 and D_2 distributions, and the modes of all three distributions are similar (Fig. A -5A). In this situation, the relative probability of grains being transported produces a similar distribution to the actual deposits. This suggests that the environment is in dynamic equilibrium and for every grain in the deposit, there is an equal probability that it will be transported and re-deposited (i.e. there is a grain by grain replacement along the transport path).
- (2) The shapes of the three distributions are similar, but the mode of X is finer than the modes of D_1 and D_2 (Fig. A -5B). In this situation, more fine grains are being deposited than are being eroded and transported; thus the environment is undergoing net accretion.
- (3) The shapes of the three distributions are similar, but the mode of X is coarser than the modes of D_1 and D_2 (Fig. A -5C). Thus, more grains are being eroded than being deposited and the environment is undergoing net erosion.
- (4) Regardless of the shapes of D_1 and D_2 , the X-distribution more or less increases monotonically over the complete size range of the deposits (Fig. A -5D). This occurs when sediment, once deposited, undergoes no further transport. The environment, therefore, is undergoing total deposition and further erosion and transport of sediment ceases.

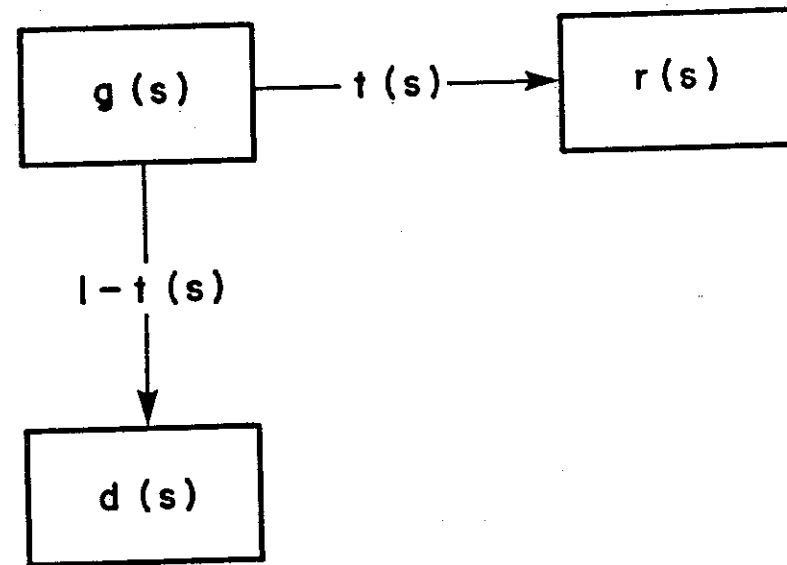


Figure A-1 : Sediment transport model to develop a lag deposit
(see Appendix **II** for definition of terms).

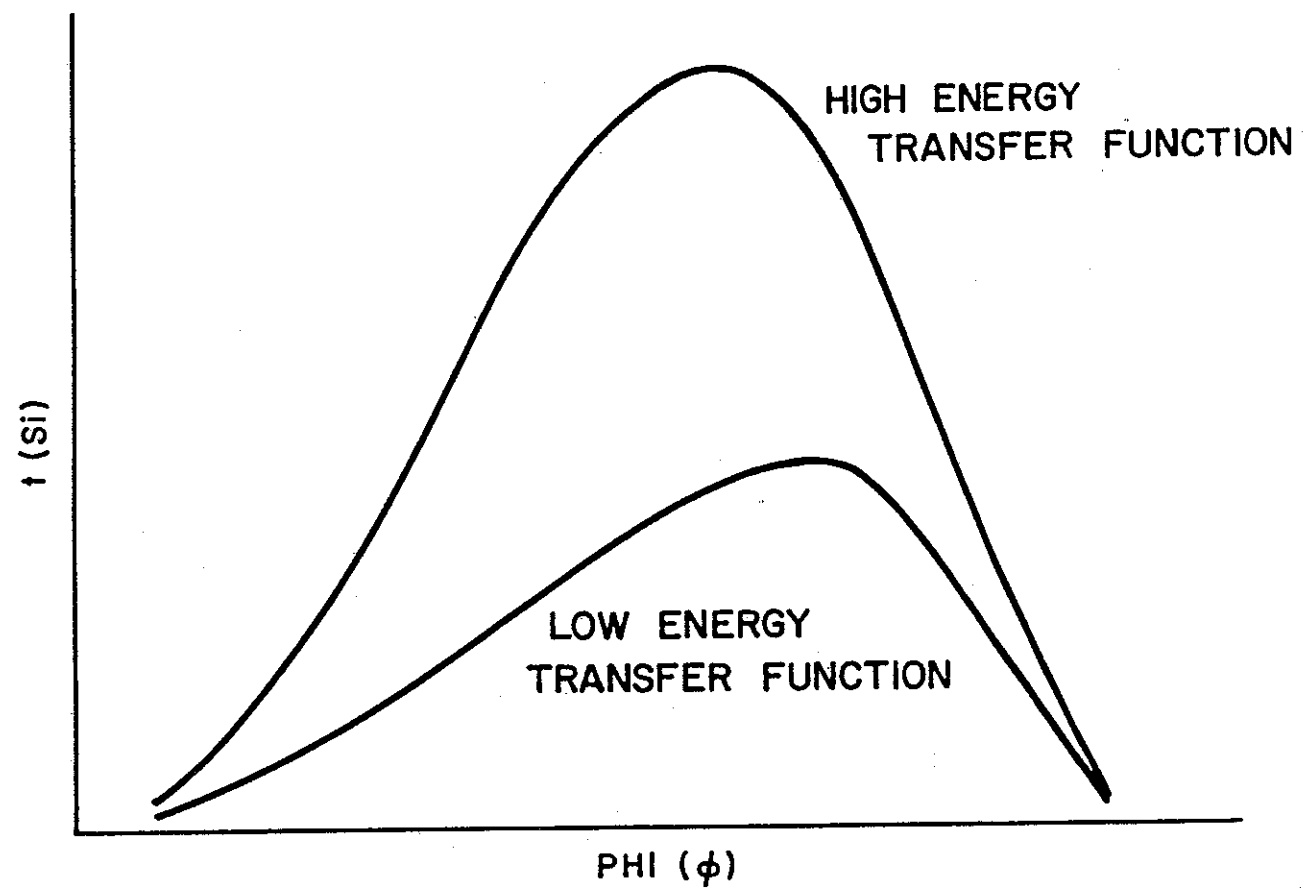


Figure A-2 : Diagram showing the extremes in shape of transfer functions $t(s)$.

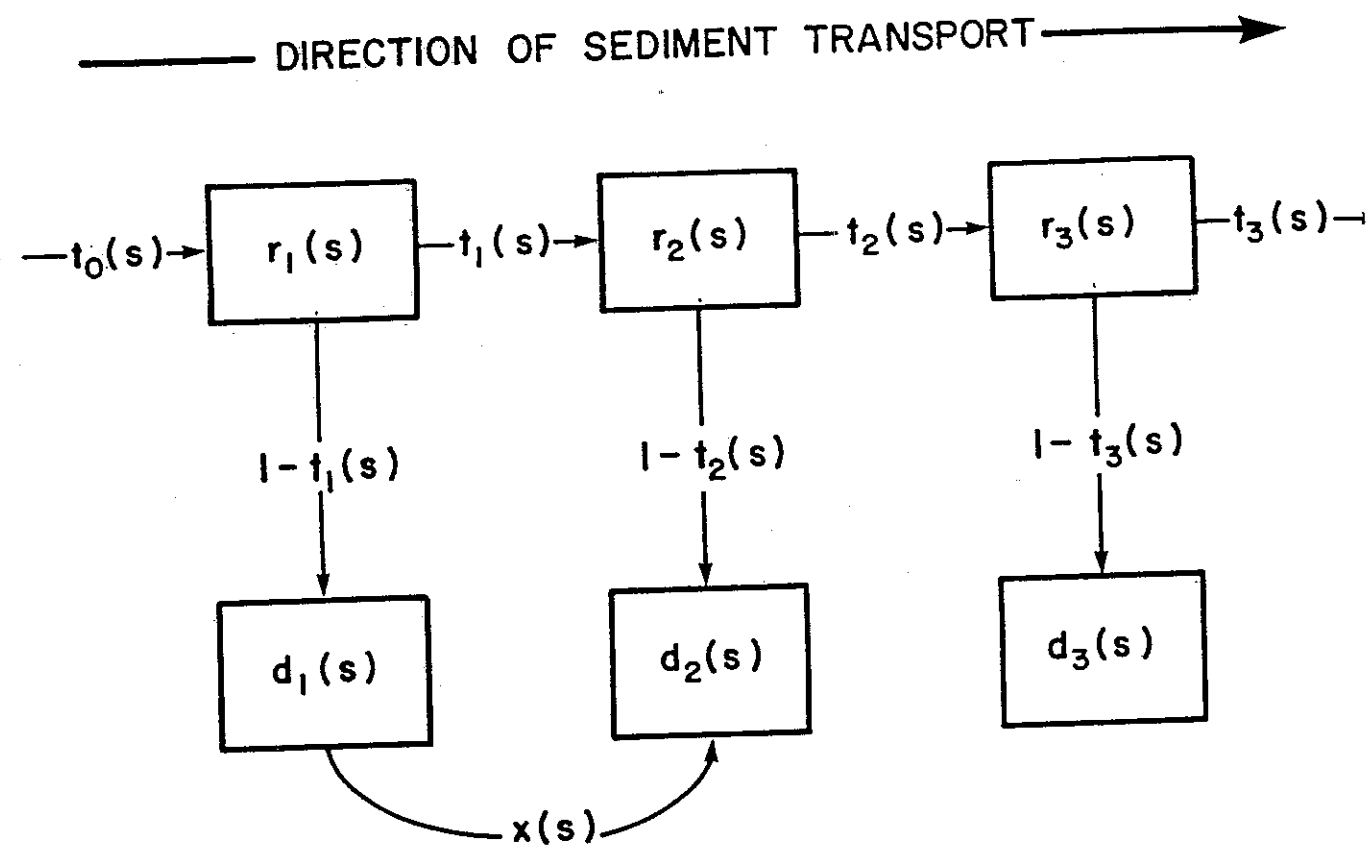
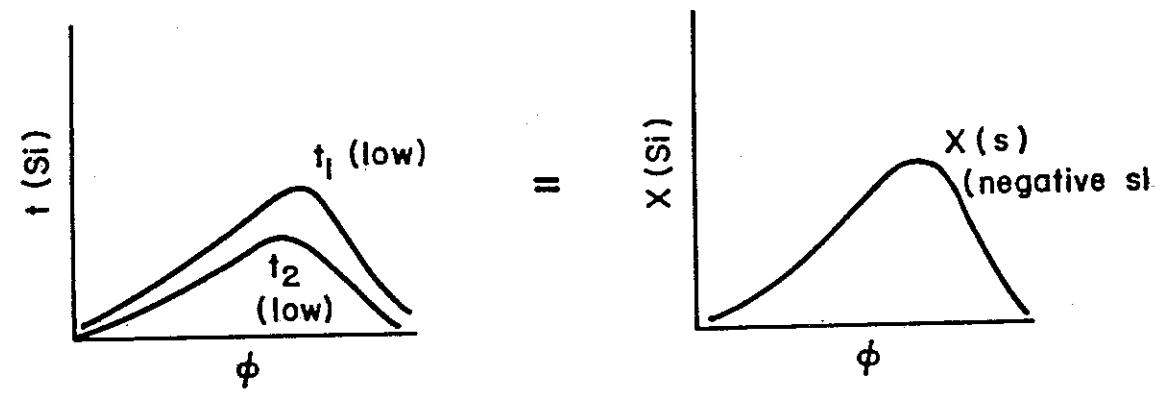


Figure A-3 : Sediment transport model relating deposits in the direction of transport (see Appendix I for definition of terms).

CASE B: $t_2 < t_1$; both low energy functions



CASE C: $t_2 < t_1$; t_1 is a high energy function; t_2 is high or low

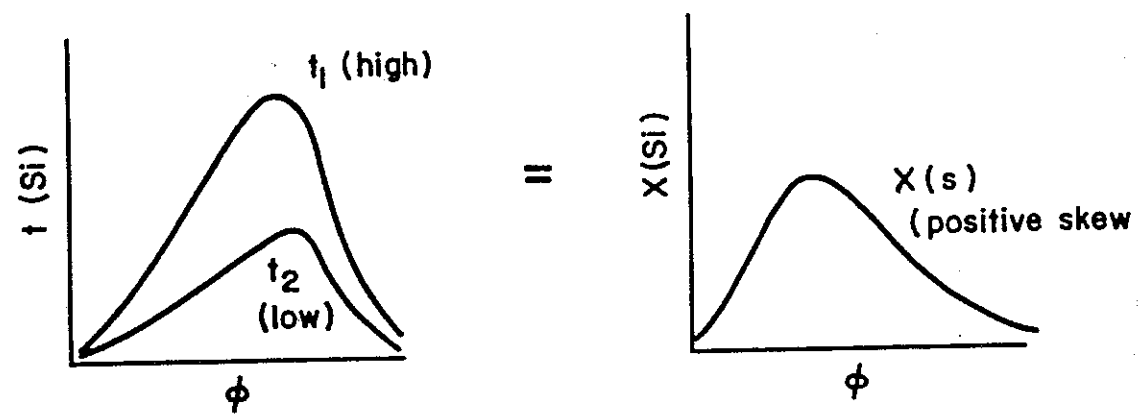


Figure A-4 : Summary diagram of t_1 and t_2 and corresponding X -distributions (equation 3) for Cases B and C (Table A-1).

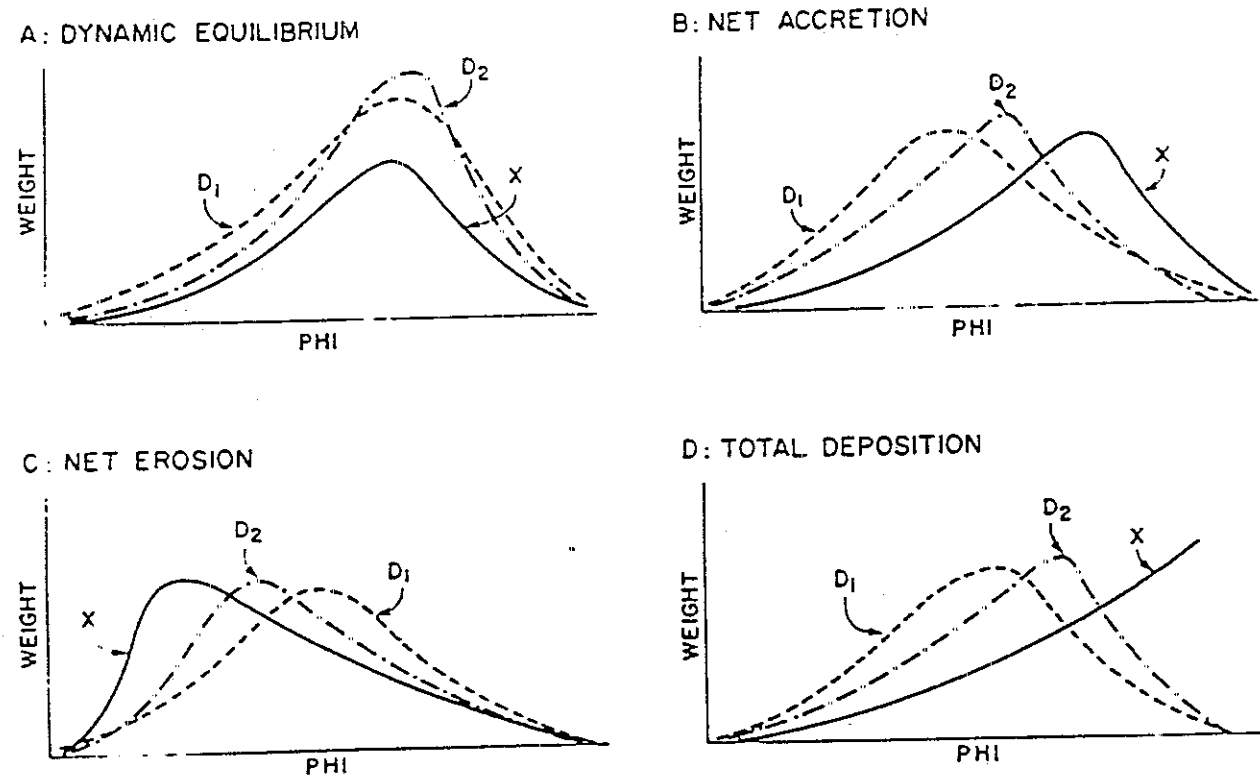


Figure A-5: Summary of the interpretations given to the shapes of X-distributions relative to the D_1 and D_2 deposits.

TABLE A-1: Summary of the interpretations with respect to sediment transport trends when one deposit is compared to another

CASE	RELATIVE CHANGE IN GRAIN-SIZE DISTRIBUTION BETWEEN DEPOSIT d_2 AND DEPOSIT d_1	INTERPRETATION
A	coarser better sorted more positively skewed	d_2 is a lag of d_1 (No direction of transport can be determined)
B	finer better sorted more negatively skewed	(i) The direction of transport is from d_1 to d_2 (ii) The energy regime is decreasing in the direction of transport (iii) t_1 and t_2 are low energy transfer functions (Figure A-5)
C	coarser better sorted more positively skewed	(i) The direction of transport is from d_1 to d_2 (ii) the energy regime is decreasing in the direction of transport (iii) t_1 is a high energy transfer function (Figure A-5) (iv) t_2 is a high or low energy transfer function